



Comparison of Predictions from the Gas Dispersion Model DRIFT (Version 3) against URAHFREP Data

ESR/D1000976/001/Issue 4

29th June 2012

Authorisation Sheet

Report Title:	Comparison of Predictions from the Gas Dispersion Model DRIFT (Version 3) against URAHFREP Data	
Customer Reference:		
Project Reference:	D1000976	
Report Number:	001	
Issue:	Issue 4	
Distribution List:		

Author:	G A Tickle	29/06/2012
Reviewed:	S A Ramsdale	29/06/2012
Authorised:	N Ketchell	29/06/2012

Comparison of Predictions from the Gas Dispersion Model DRIFT (Version 3) against URAHFREP Data

Gemma Tickle, Darshana Godaliyadde and James Carlisle
ESR Technology Ltd
Whittle House
410 The Quadrant
Birchwood Park
Warrington
WA3 6FW

The dense gas dispersion model DRIFT has recently been extended to include the modelling of buoyant lift-off and rise. A major motivation of this extension is the modelling of hydrogen fluoride (HF) clouds in low wind, humid conditions. This report presents comparisons of predictions using the extended DRIFT model (designated DRIFT Version 3) against data obtained from the EU URAHFREP research project. DRIFT model predictions are compared against URAHFREP wind-tunnel data for ground-level buoyant plume and puff sources. Comparisons are also made against URAHFREP field trials data for HF releases. Checks of DRIFT's HF thermodynamic model predictions against experimental data and previous model versions are included. The comparisons indicate that the extended model generally gives a good representation of the effect of buoyancy on maximum concentration, and the buoyancy at which lift-off occurs, although the ground-level concentration may be over-predicted when the cloud has significantly lifted from the ground. Example runs for 1 kg/s HF releases demonstrate the ability of DRIFT Version 3 to predict HF dispersion for a much wider set of atmospheric conditions than was possible with Version 2 – with a significant shortening of hazard range under conditions where buoyant lift-off is predicted.

This report and the work it describes were funded by the Health and Safety Executive. Its contents, including any opinions and/or conclusions expressed, are those of the authors alone and do not necessarily reflect HSE Policy.

CONTENTS

CONTENTS	ii
1 INTRODUCTION	1
2 COMPARISONS WITH WIND-TUNNEL DATA	2
2.1 BUOYANT PLUMES	2
2.2 BUOYANT PUFFS	7
2.3 ASYMPTOTIC BUOYANT RISE	11
3 HF THERMODYNAMIC MODEL COMPARISONS	13
3.1 SCHOTTE EXPERIMENTS	13
3.2 URAHFREP THERMODYNAMIC EXPERIMENTS	14
4 HF FIELD TRIAL COMPARISONS	18
4.1 DRIFT PREDICTIONS	18
5 SENSITIVITY TO RELATIVE HUMIDITY	20
6 CONCLUSIONS	24
6.1 COMPARISONS WITH WIND-TUNNEL DATA	24
6.2 COMPARISONS WITH HF THERMOYNAMICS DATA	24
6.3 COMPARISONS WITH FIELD TRIALS DATA	25
6.4 SENSITIVITY TO RELATIVE HUMIDITY	25
6.5 CONCLUDING REMARKS	25
7 REFERENCES	26
APPENDICES	27
APPENDIX 1 BUOYANT PLUME GRAPHS	28
APPENDIX 2 BUOYANT PUFF GRAPHS	43

1 INTRODUCTION

The DRIFT (Dispersion of Releases Involving Flammables or Toxics) gas dispersion model has recently been enhanced. The modelling enhancements include:

- Dispersion of buoyant clouds, including buoyant lift-off and rise
- Modelling upwind spreading at the source for continuous dense releases
- Multi-component mixtures
- Time-varying dispersion
- Use of HSE substance property (SPI) files

The new software implementation of the DRIFT incorporating these enhancements is designated DRIFT Version 3. The model equations for DRIFT Version 3 are documented in [2].

A major motivation for the DRIFT enhancements is improved modelling of the atmospheric dispersion of hydrogen fluoride (HF) from possible accidental releases. HF thermodynamic models suggest that, under low wind, humid conditions, initially dense HF clouds may become sufficiently buoyant for the clouds to partially or completely lift-off from the ground giving significantly reduced ground-level concentrations. HF thermodynamics and lift-off of initially ground-based buoyant clouds was studied under the EU research project called URAHFREP conducted between the years 1997-2001 [3]. The findings of the URAHFREP project guided the DRIFT enhancements recommended in [1].

This report presents comparisons of DRIFT Version 3 model predictions with experimental data obtained during the URAHFREP project. The focus of these comparisons is validating and verifying¹ the URAFHREP related enhancements to the DRIFT model. The comparisons cover:

- Dispersion, lift-off and rise predictions compared with wind-tunnel data for ground-level buoyant sources
- HF thermodynamic model predictions with laboratory scale data
- Dispersion predictions compared with URAHFREP HF field trial data.
- Comparisons with DRIFT Version 2 and sensitivity of lift-off to relative humidity.

Other comparisons of DRIFT Version 3 with DRIFT Version 2 and non-buoyant aspects are presented elsewhere [3].

¹ We distinguish between verification which involves checking that the software implementation matches the intended mathematical model equations and validation which covers determining the ability of the model equations to represent observed reality.

2 COMPARISONS WITH WIND-TUNNEL DATA

As part of the URAHFREP project, BRE undertook wind-tunnel modelling on buoyant gas dispersion from ground-level sources – both steady continuous and short duration (puff) releases were modelled. Details of these wind-tunnel experiments are given in refs [6] and [7]. Data from the experiments are also included as part of the REDIPHEM database [8]. Ref [5] compared the results from the steady continuous wind-tunnel releases with predictions simple plume models – these comparisons informed the proposed buoyant extensions to DRIFT recommended in ref [1]. DRIFT Version 3 includes buoyant extensions based upon the recommendations in [1]. Ref [2] gives details of the mathematical model implemented in DRIFT Version 3. In the following sections we present comparisons of DRIFT version 3 predictions with the URAHFREP wind-tunnel data for buoyant plumes [6] and buoyant puffs [7].

2.1 BUOYANT PLUMES

2.1.1 Experimental Conditions

The buoyant plume wind-tunnel experiments [6] varied buoyancy flux, source dimensions and shape. The different source geometries modelled are given in Table 2.1 and show schematically in Figure 2-1. The simulated rough-wall boundary layer was equivalent to an aerodynamic roughness height z_0 of $0.029L$ (i.e. $z_0/L=0.029$). Following [6], all lengths are non-dimensionalised by dividing by a reference length scale, L (6.7cm).

Table 2.1 Source dimensions

<i>Group</i>	<i>Identifying Letter</i>	<i>Width y/L</i>	<i>Length x/L</i>	<i>Area xy/L²</i>
Square Sources	A	0.448	0.448	0.2
	B	1.19	1.19	1.4
	C	2.69	2.69	7.2
	D	3.43	3.43	11.8
	E	6.87	7.16	49.2
Wide Sources	G	0.448	3.43	1.54
	H	1.19	3.43	4.10
	D	3.43	3.43	11.78
	I	7.16	3.43	24.59
	J	14.33	3.43	49.19
Long Sources	K	28.66	3.43	98.37
	F	3.43	0.448	1.54
	L	3.43	1.19	4.10
	D	3.43	3.43	11.78
	M	3.43	7.16	24.59
	N	3.43	14.33	49.19
	P	3.43	28.66	98.37

Source buoyancy for the releases is expressed via the dimensionless buoyancy flux defined as

$$\frac{F}{u^3 L} \quad (1)$$

where the (dimensional) buoyancy flux is, F , is:

$$F = \frac{g}{\pi} V \frac{\Delta\rho}{\rho_a} \quad (2)$$

g is the acceleration due to gravity
 u is the wind speed at reference height L
 V volumetric release rate from source

$\frac{\Delta\rho}{\rho_a} = \frac{\rho_a - \rho}{\rho_a}$ is the relative density difference between ambient ρ_a the source ρ

The dimensionless buoyancy flux values used in the experiments and their identifying codes are shown in Table 2.2.

Table 2.2 Dimensionless buoyancy flux values

<i>Identifying Code</i>	<i>Dimensionless Buoyancy Flux F/u^3L</i>
S	<0.001
T	0.003
U	0.01
V	0.03
W	0.1
X	0.3
Y	1.0
Z	3.0

Concentration measurements were made at fixed locations shown in Figure 2-1. The concentrations were presented in the dimensionless form, K defined by:

$$K = \frac{cuL^2}{Q} \quad (3)$$

where c measured volumetric concentration
 u reference wind speed at the reference height L
 Q volumetric rate of discharge of the tracer

The experimental conditions used to generate the range of dimensionless buoyancy fluxes in Table 2.2 are shown in Table 2.3.

Table 2.3 Experimental release conditions

<i>Buoyancy Condition</i>	<i>S</i>	<i>T</i>	<i>U</i>	<i>V</i>	<i>W</i>	<i>X</i>	<i>Y</i>	<i>Z</i>
Reference Wind Speed (ms ⁻¹)	1	1	1	0.5	0.5	0.4	0.4	0.32
Total Volume Discharge (m ³ s ⁻¹)	1.67x10 ⁻⁵	9.17x10 ⁻⁵	2.67x10 ⁻⁴	1.10x10 ⁻⁴	3.27x10 ⁻⁴	4.97x10 ⁻⁴	1.62x10 ⁻³	2.45x10 ⁻³
Buoyancy Flux, F	2.3x10 ⁻⁵	2.3x10 ⁻⁴	6.9x10 ⁻⁴	2.7x10 ⁻⁴	8.6x10 ⁻⁴	1.3x10 ⁻³	4.3x10 ⁻³	6.6x10 ⁻³
Dimensionless Buoyancy Flux, F/u ³ L	0	0.003	0.01	0.03	0.1	0.3	1	3

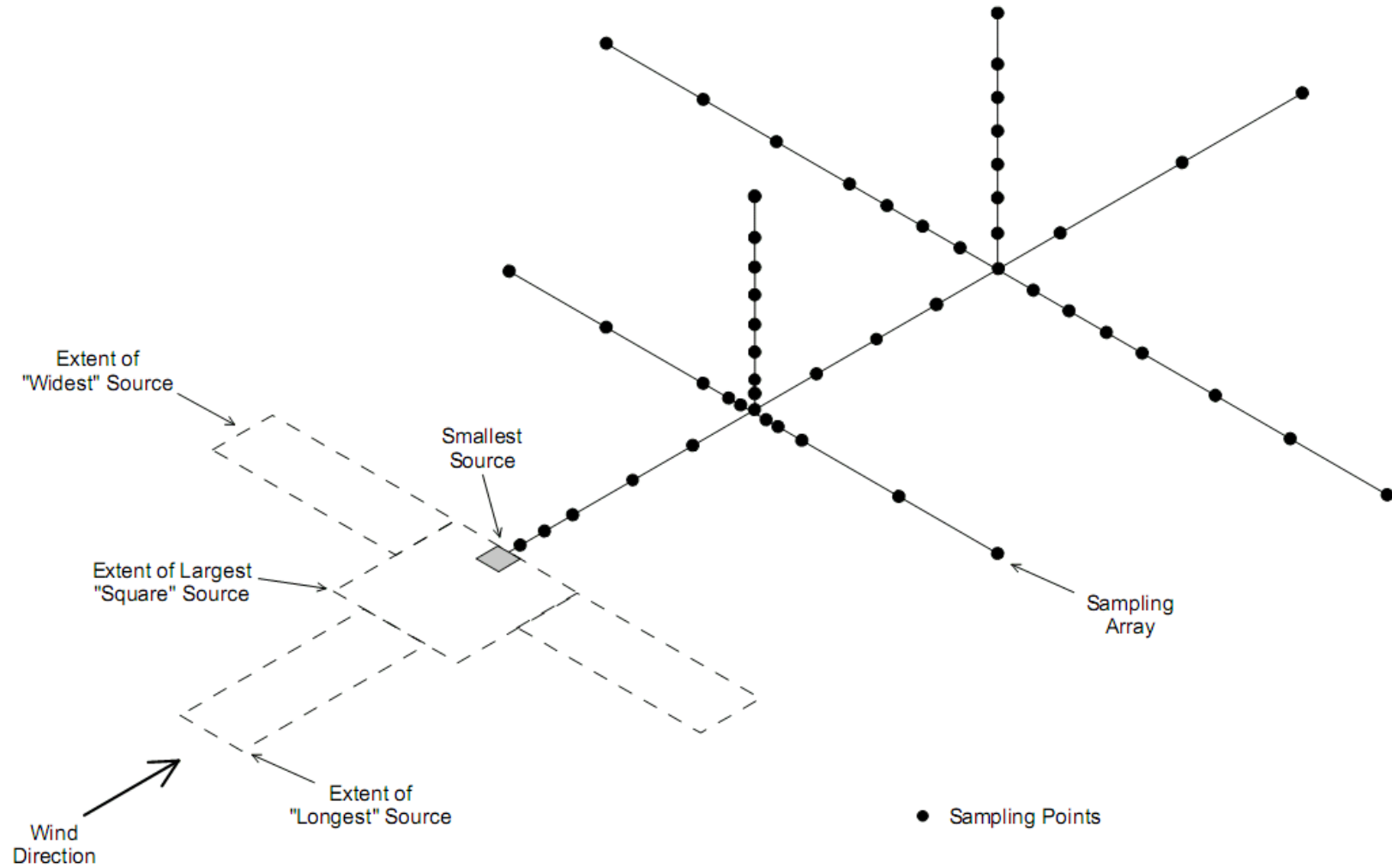


Figure 2-1 Layout of concentration sampling array used in wind-tunnel experiments

2.1.2 DRIFT Predictions

The wind-tunnel plume releases have been modelled using DRIFT Version 3.6.1. The DRIFT modelling has been undertaken at the wind-tunnel scale with the non-dimensional buoyancy fluxes in Table 2.2 achieved by matching the wind speed and volumetric flux in Table 2.3 and adjusting the molecular weight of the release material. Due to the absence of significant temperature gradients in the wind-tunnel boundary layer flow, neutral atmospheric stability is assumed. To avoid the complications of interaction of the plume with an elevated inversion in DRIFT modelling, the boundary layer height for the DRIFT runs was set to a height of 10 m (i.e. significantly above the heights of the wind-tunnel measurements).

DRIFT's low momentum area source model has been used for the runs [2, 9]. This source model permits elliptical rather than rectangular source shapes. The wind-tunnel sources have therefore been approximated by matching the source area and also matching the ratio of the downwind to cross-wind source extents.

DRIFT concentration predictions have been non-dimensionalised following equation (3). The following quantities have been extracted from the DRIFT predictions for the two vertical sampling array positions of $x/L = 14.9$ and $x/L = 29.8$:

- K_{max} : the maximum centreline concentration over the wind-tunnel measurement height
- K : the ground-level centreline concentration
- Z_c/L : the height of the maximum concentration K_{max}

The DRIFT predictions are compared with parametric fits [6] to the wind-tunnel results. DRIFT predictions for all the sources types are shown graphically in Appendix 1. These graphs show how non-dimensional buoyancy flux affects the predicted concentrations and plume rise for each source and also how this compares with the wind-tunnel results.

As an example, the predictions for Source C (square source with area $7.2L^2$) are shown below in Figure 2-2. The wind-tunnel variation of maximum concentration K_{max} decreasing with buoyancy is well matched by DRIFT. The height of the maximum Z_c/L is reasonably well represented, with some degree of underprediction at the highest buoyancies. The ground-level concentration is well reasonably represented up to a non-dimensional buoyancy flux of approximately 0.1, after which DRIFT predicts significantly higher ground-level concentrations than from the wind-tunnel parametric fits.

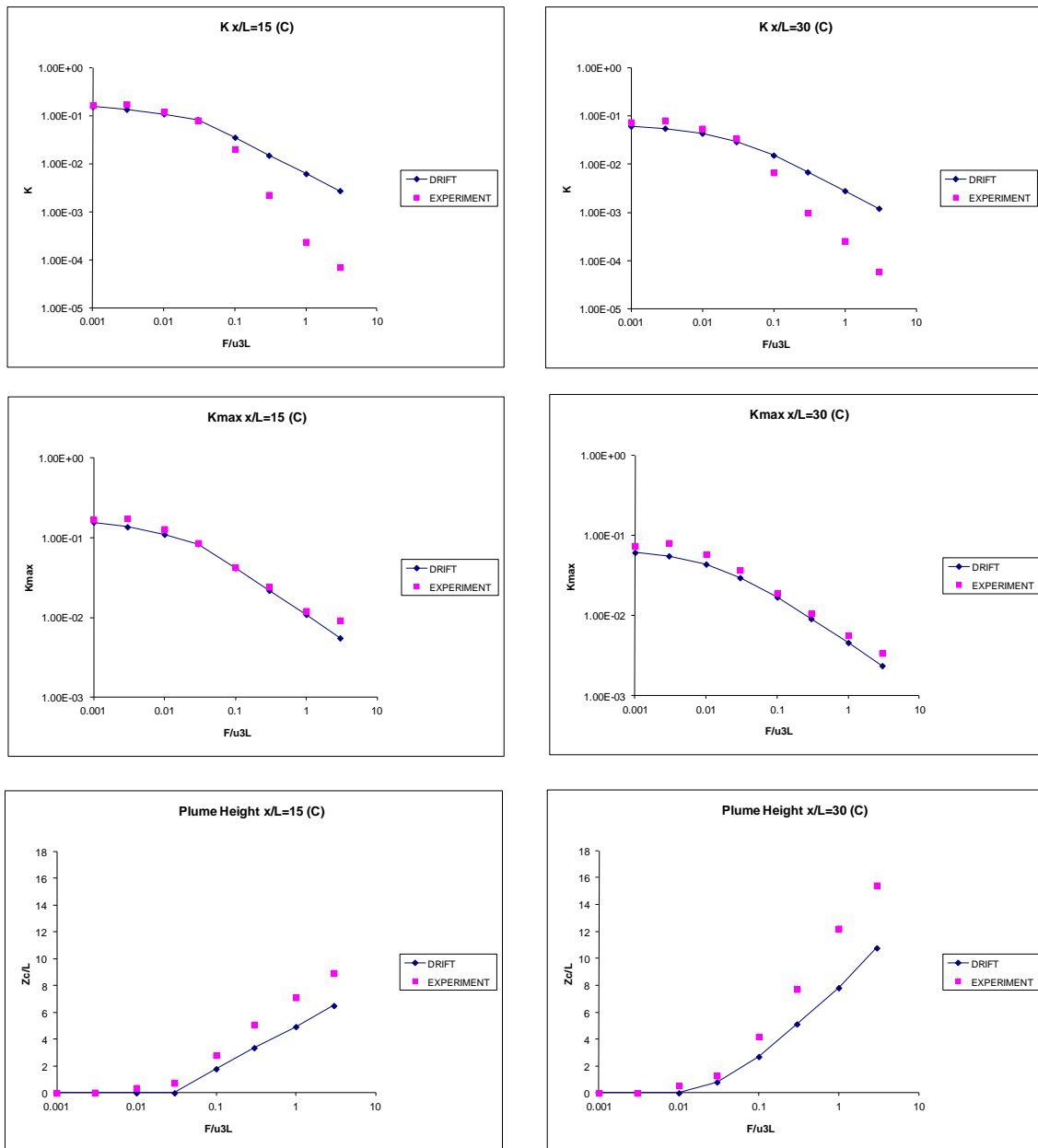


Figure 2-2 DRIFT predictions for plume source C

The above observations for Source C appear to generally apply, with some exception noted below, to the other source sizes and shapes. We infer the following from comparisons in Appendix 1:

- The good agreement of K_{max} suggests that the entrainment model used in DRIFT adequately represents the effect of increasing buoyancy on rate of dilution. The simple modelling in [5] suggested that this might be the case – it is reassuring to see this confirmed from the more complicated equation set implemented in DRIFT Version 3.
- Comparison of the of plume height Z_c/L variation with buoyancy between DRIFT and experiment suggests that the buoyancy at which the maximum concentration starts to rise from the ground is reasonably well predicted by DRIFT for most source geometries. Even the lift-off transition buoyancy for ‘Wide Sources’ appears to be reasonably well predicted. This indicates that DRIFT is performing better at including the effects of source size on lift-off than the ‘critical lift-off parameter approach’ and simple plume

models investigated in [5]. A notable exception is the behaviour for the longest ‘Long Source’, Source P, we discuss separately below.

- For the longest ‘Long Source’, Source P, DRIFT predicts Z_c/L as being zero at the closest vertical array, whereas the wind-tunnel data suggest lift-off elevation for non-dimensional buoyancy flux of 0.03 at higher. Ref [6] noted that for this source buoyant lift-off was apparently enhanced. This is possibly due to earlier buoyant rise from the upwind side of the source and the additional effect of buoyancy being added from the rest of the source – this is in contrast with DRIFT which treats the plume cross-section from the source as an ‘integral’ entity which due to bending of the plume trajectory remains in contact with the ground at the closest measurement array.
- The plume height Z_c/L predictions from DRIFT are with zero ‘added mass’ in the plume vertical momentum equation. Including added mass was found to be detrimental to the agreement with the wind-tunnel data, with added mass suppressing too much the buoyant rise.
- The ground-level concentration, K , from lifted-off plumes is generally predicted to be larger from the DRIFT runs than indicated by the wind-tunnel parametric fits. In some cases this difference can be greater than an order of magnitude. This may indicate that, at least on the vertical centreline plane, the plume is more compact than predicted by DRIFT. This could be the result of the buoyant rising plume developing a ‘kidney’ shape cross-section, whereas DRIFT is asymptotically tending to an axi-symmetric cross-section. The good agreement for K_{max} from DRIFT suggests that the overall plume cross-sectional area is reasonably well represented. Sensitivity calculations in DRIFT suggest that there would be little improvement in ground-level predictions by keeping Gaussian shaped profiles for the entirety of the run (normally DRIFT smoothly transitions to the ground-based passive plume value of $s = 1$ for neutral atmosphere). Another factor that may contribute to the some of the observed difference is the displacement of the ground-level maximum laterally from the centre-line which occurred for some of the wind-tunnel measurements. Also, it is possible that, at very low concentrations, the parametric fits may not always accurately represent the actual maximum ground-level concentration.

2.2 BUOYANT PUFFS

2.2.1 Experimental Conditions

The buoyant puff wind-tunnel experiments [7] investigated lift-off and dispersion behaviour of short duration buoyant releases. The experiments were undertaken in the same wind-tunnel as the plume experiments [6]. Release duration was varied in addition release buoyancy and source shape. Many repeat experiments were required for the buoyant puff releases to due to the inherent variability of puff dispersion.

Three different kinds of sources were implemented for the puff experiments, namely long (G), square (D) and wide (J). The dimensions and identifying letters are given in Table 2.4. The same length scale ($L=6.7\text{cm}$) is adopted for non-dimensionalisation as in the plume experiments.

Table 2.4 Source description

<i>Identifying Letter</i>	<i>Width y/L</i>	<i>Length x/L</i>	<i>Area xy/L²</i>
G	0.448	3.43	1.54
D	3.43	3.43	11.78
J	14.33	3.43	49.19

The discharge conditions used for the puff releases are shown in Table 2.5.

Table 2.5 Puff Release Discharge Conditions

<i>Release Identifier</i>	<i>F/u³L</i>	<i>Release Duration, T (s)</i>	<i>Dimensionless Release Duration, uT/L</i>	<i>Release Volume V_p (ml)</i>	<i>Dimensionless Release Volume, V/L³</i>	<i>Wind Speed, u (ms⁻¹)</i>
A	0 and 3	0.8	4	2000	6.7	0.32
B	0 and 3	0.2	1	500	1.7	0.32
C	0 and 0.1	0.4	3	130	0.4	0.5
D	0 and 0.1	0.16	1	50	0.17	0.5

The same concentration measurement array as for the plumes (see Figure 2-1) was used.

2.2.2 DRIFT Predictions

The wind-tunnel puff releases have been modelled using DRIFT Version 3.6.1. As for the plume cases, the DRIFT modelling has been undertaken at the wind-tunnel scale, this time using the release conditions in Table 2.5.

The puff releases were modelled in DRIFT using two alternative approaches:

- **Finite Duration Release** The release is modelled as a low momentum area source which is approximated as being steady and continuous over the release duration. DRIFT accounts for the finite duration by including additional longitudinal dispersion (mixing at the front and back edges of the plume segment).
- **Instantaneous Release** The entire release volume is modelled as being instantaneously released puff. DRIFT's puff model includes longitudinal as well as lateral dispersion.

For the finite duration releases, the non-dimensional buoyancy fluxes in Table 2.5 were achieved by matching the wind speed and volumetric flux and adjusting the molecular weight of the release material. For the instantaneous releases the same molecular weights were used, together with the matching the total release volume.

The wind-tunnel boundary layer flow was modelled as for the plume runs, matching to the wind speeds in Table 2.5.

As for the plumes, DRIFT's elliptical source model has been used to approximate the rectangular wind-tunnel source shapes by matching the source area together with the ratio of the downwind to cross-wind source extents.

DRIFT concentration (% vol/vol) predictions have been compared with the wind-tunnel puff results. The following quantities have been compared for the two vertical sampling array positions of $x/L = 14.9$ and $x/L = 29.8$:

- *C_{max}*: the maximum centreline concentration over the wind-tunnel measurement height range
- *C*: the ground-level centreline concentration
- *Z_{max}/L*: the height of the maximum concentration *C_{max}*

The DRIFT predictions are compared with maximum measured concentrations from the wind-tunnel [7]. Graphs of the predictions for all puff sources are given in Appendix 2. These graphs

show how the DRIFT predictions vary with non-dimensional buoyancy flux and release duration and how this variation compares with the wind-tunnel results. In these comparisons, the large variability of the wind-tunnel results should be born in mind.

As an example comparison, Figure 2-3 and Figure 2-4 illustrate the DRIFT predictions for Source D. The x-axis labels in these figures indicate firstly the release identifier (codes A-D in Table 2.5) and secondly the buoyancy condition (A, Z and W in Table 2.2).

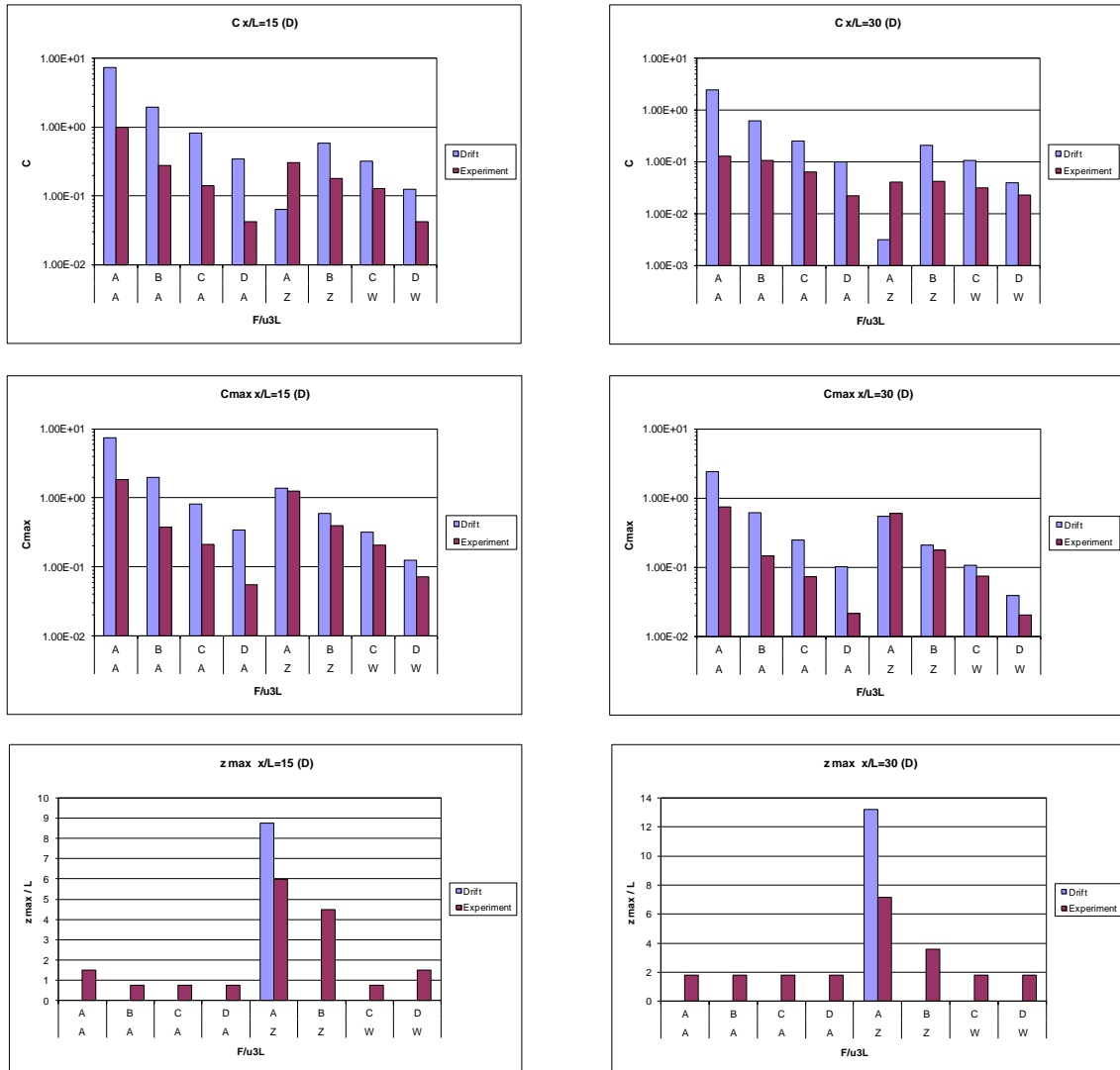


Figure 2-3 DRIFT finite duration model predictions for puff source D

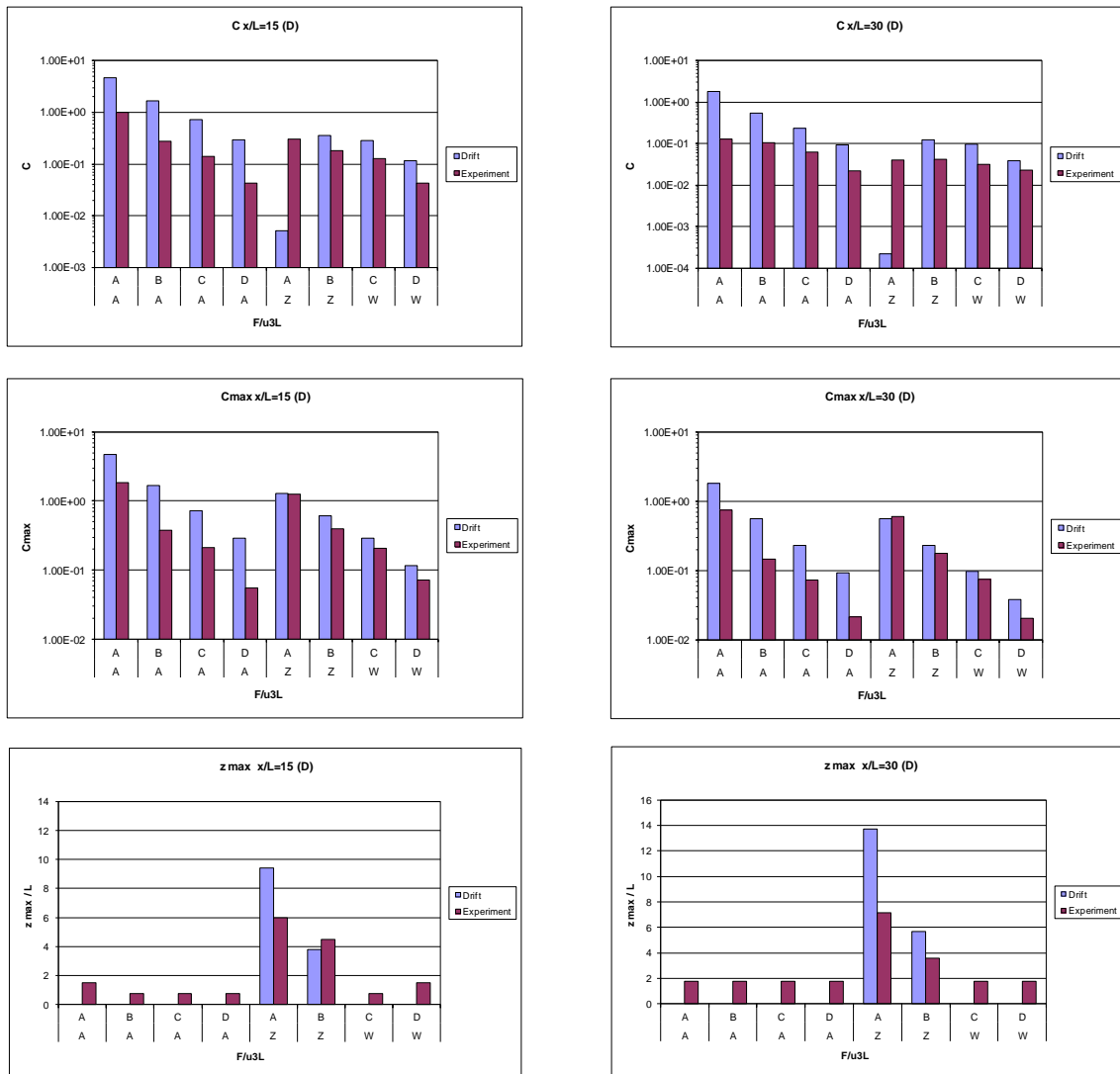


Figure 2-4 DRIFT instantaneous model predictions for puff source D

From the above results for source D together with the other results shown in Appendix 2, we make the following general observations:

- In general the C_{max} predictions are similar for releases modelled using the finite duration and instantaneous models. This implies that the main scaling behaviour comes from the total buoyancy (buoyancy flux multiplied by release duration) of the released material rather than buoyancy flux.
- Generally, the variation of C_{max} with buoyancy (and duration) for each source (G, D and J) is reasonably well represented by DRIFT. The variation also reflects the expected qualitative trends that:
 - Decreasing the release duration decreases C_{max} .
 - Increasing the release buoyancy also decreases C_{max} .
- The wind-tunnel data for Z_{max}/L indicates that puff rise is generally much lower than from a continuous plume release with the same dimensionless buoyancy flux. For the puff releases only the highest buoyancy conditions Z gives significant lift-off, whereas for the continuous releases, lift-off was observed at lower buoyancy conditions (fluxes). DRIFT predictions also show this, however in general the DRIFT predictions slightly overpredict buoyant rise for release condition A (longest duration release) in combination with the highest buoyancy condition Z.

- Some momentum induced lift-off is evident in the wind-tunnel data, even for zero buoyancy condition A, this is not present in the DRIFT runs which neglect momentum at the source.
- Although the finite duration and instantaneous model are found to predict similar C_{max} values, they may differ in their Z_{max}/L predictions; with the instantaneous model generally giving lift-off at lower buoyancy conditions, in better overall agreement with the wind-tunnel observations.
- In general the ground-level concentration predictions from DRIFT follow the Z_{max}/L predictions in that:
 - Where there is no lift-off the agreement is generally good, reflecting the good predictions for C_{max} .
 - Where Z_{max}/L is overpredicted by DRIFT as for high buoyancy, there is some tendency for the model to underpredict ground-level concentrations.
 - Where there is momentum induced lift-off which is precluded by DRIFT's low momentum source assumption then ground-level concentrations are generally overpredicted.

2.3 ASYMPTOTIC BUOYANT RISE

The buoyant puff rise model incorporated into DRIFT is based on a generalisation of the integral model of Turner [10]. As a check on the computer implementation in DRIFT, it is instructive to compare DRIFT puff rise predictions with an analytic solution to Turner's model. Following the approach given in [11] the asymptotic rise of the puff centre height, z_m , as a function of time, t , in zero wind is given by

$$z_m = \alpha^{-3/4} B^{1/4} t^{1/2} \quad (4)$$

where

$$B = \frac{g}{\pi} \frac{\rho_a - \rho}{\rho_a} V_s \quad \text{is the buoyancy for a puff release of volume } V_s$$

and α is an entrainment coefficient with value of approximately 0.25. As well as assuming zero wind the above formula assumes a ground-level point source with zero momentum.

Figure 2-5 shows DRIFT predictions for the puff source D from the wind-tunnel experiments [7] with different buoyancy conditions for the original 0.32 m/s, and also for a much lower wind speed² of 0.005 m/s. Also shown in Figure 2-5 is a green line corresponding to equation (4). It can be seen that in general DRIFT shows very similar asymptotic at low wind. The effect of a higher wind is, as expected and observed in the wind-tunnel experiments, to reduce the puff rise to below the asymptotic form given above.

Since DRIFT's buoyant puff equations are based on a generalisation of Turner's model this comparison is best viewed as a verification check on DRIFT's computer implementation, rather than validation against independent data. However, the complexities of the generalisation in DRIFT make such a check worthwhile.

² DRIFT cannot model dispersion in exactly zero wind speed, but very low wind speeds e.g. 0.005 m/s can be input.

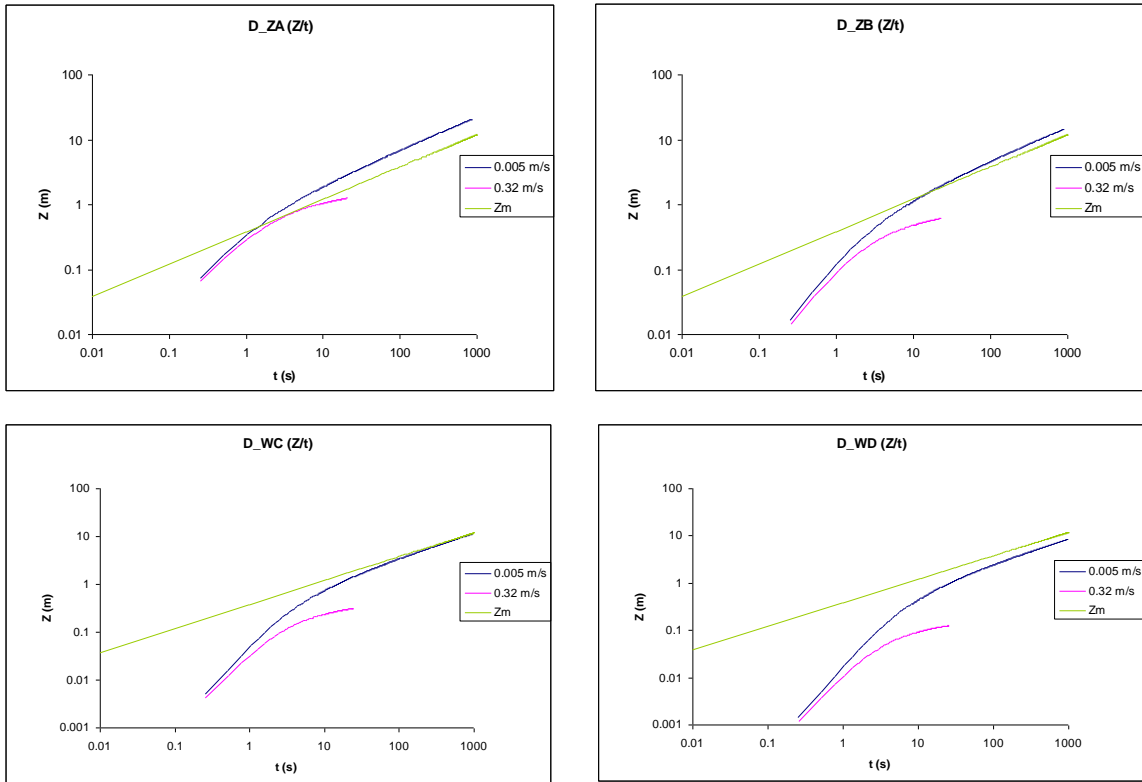


Figure 2-5. DRIFT predictions of puff rise from puff source D in 0.32 m/s and 0.005 m/s wind compared with analytic prediction Z_m

3 HF THERMODYNAMIC MODEL COMPARISONS

The thermodynamic model in DRIFT Version 3 extends that in DRIFT Version 2 by allowing for modelling of multi-component mixtures. The multi-component mixture model in DRIFT allows the specification of distinct (mutually immiscible) liquid phases, each distinct liquid phase may itself be an ideal mixture of components, or in the case of hydrogen fluoride–water and ammonia–water systems non-ideal interacting mixtures. Additionally DRIFT Version 3, as for Version 2, includes modelling of HF associations (oligomers) in the vapour phase using an approach based upon [13].

One of the aims of generalising DRIFT's thermodynamic model to multi-components is to allow modelling of dispersion of HF-hydrocarbon mixtures as might possibly occur from HF alkylation separators. The presence of hydrocarbon aerosol (e.g. iso-butane liquid) may counteract the buoyancy generation in an HF cloud mixing with moist air. Extension of DRIFT's HF-model to include immiscible components was proposed in [12]. A spreadsheet implementation (HF-Mixture) of this model was used in [12] to compare with the original HF-moist air data of Schotte [14] and with new HF thermodynamic data including iso-butane-HF-moist air mixtures [15].

To simplify the computer implementation for multi-component mixtures, the thermodynamic modelling in DRIFT Version 3 is based on solving implicit equations for thermodynamic equilibrium, HF oligomer formation and mixture enthalpy in parallel with the differential equations for the cloud dispersion [2]. This differs from the computational approach in DRIFT Version 2 which used a differential form for all the equations.

As a check on the coding in the DRIFT Version 3, we repeat the comparisons in [12]. DRIFT Version 3.1.1 has been used for these comparisons.

3.1 SCHOTTE EXPERIMENTS

Schotte [14] reported the temperature change on mixing HF vapour with moist air in a fog chamber for a range of relative humidities. All streams were initially at the same temperature of 299K. Figure 3-1 shows the temperature predictions for these experiments using DRIFT Version 3. Also shown in Figure 3-1 are the experimental data and the HF-Mixture model predictions from [12]. The DRIFT Version 3 predictions match almost exactly those from the HF-Mixture model and are also in excellent accord with the experimental measurements of Schotte.

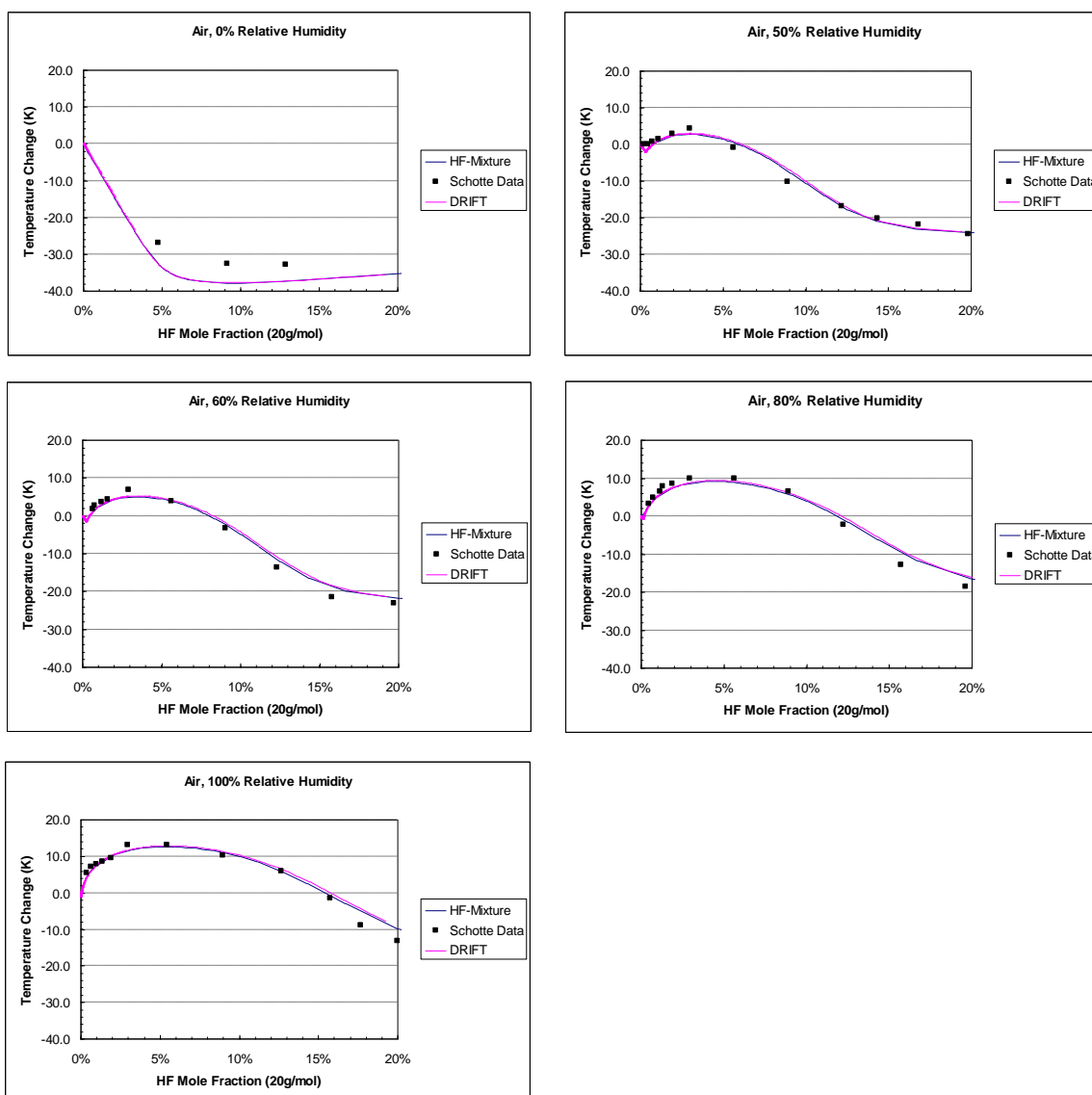


Figure 3-1 Temperature change on mixing HF with moist air at 299K – Schotte Data

3.2 URAHFREP THERMODYNAMIC EXPERIMENTS

3.2.1 HF in Moist Air

HF thermodynamic mixing experiments were undertaken under URAHFREP with the aim of extending the range beyond Schotte's [14] and investigating the effects of including iso-butane in the mixture. Details of these URAHFREP thermodynamics experiments are reported in [15]. The mixed streams were initially at a temperature of 294K.

Figure 3-2 shows DRIFT predictions compared with the URAHFREP HF –moist air mixing data [15]. Again the DRIFT predictions very much match those of the HF-Mixture model in [12]. The model predictions also agree reasonably well with the experimental measurements, in particular the minimum and maximum temperatures agree well, despite the experimental measurements showing some deviations and scatter.

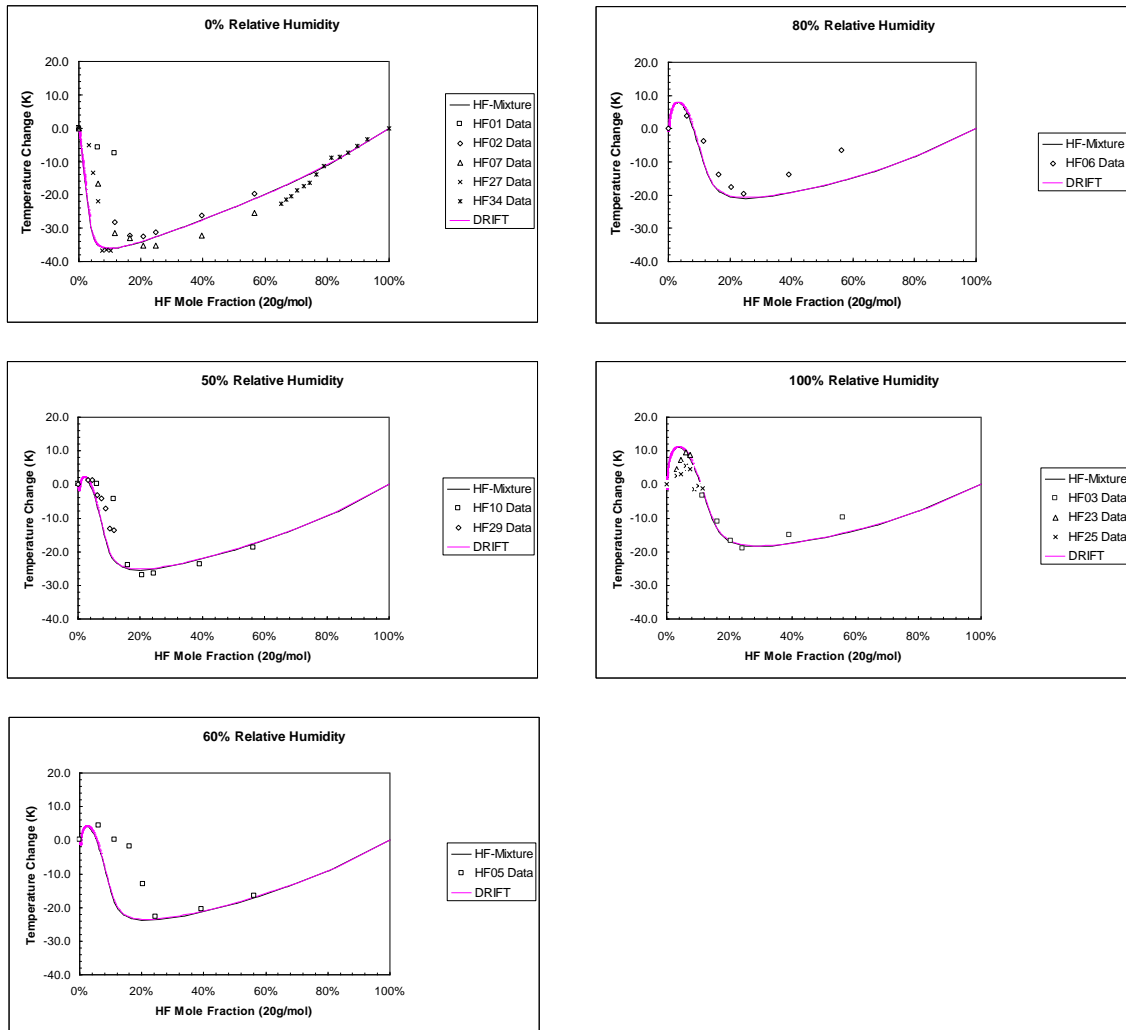


Figure 3-2 Temperature change on mixing HF with moist air at 294K – URAHFREP Data

3.2.2 HF and Iso-Butane in Moist Air

The HF-butane-moist air mixture experiments in [15] involved mixing of a vapour HF stream with a moist iso-butane and air stream. This mixing maintains a constant iso-butane water and air ratio which is difficult to obtain using a dispersion model such as DRIFT which assumes mixing of released material (which might be a mixture of HF and iso-butane), with moist air. Hence in the DRIFT dispersion modelling, in the absence of different deposition rates, the ratio HF to iso-butane would remain fixed. The HF-Mixture model used in [12] is purely a thermodynamic model which does not have these dispersion model ‘limitations’. The HF-Mixture model was found in [12] to agree well with the URAHFREP data for HF-butane mixtures. Therefore it is useful to compare DRIFT Version 3 model predictions with HF-Mixture predictions for HF-butane mixing in moist air - close agreement of the models would act as verification of the coding in DRIFT and also lend support to the validity of DRIFT when applied to HF-butane mixtures.

We compare results of DRIFT with HF-Mixture for a theoretical flashing release of HF and iso-butane. The following release conditions are considered:

- Initial mixture fractions:
 - 50% HF, 50% iso-butane by mass.
 - 100% HF
 - 100% iso-butane

- Initial mixture temperature 300 K
- Air temperature 294 K
- Air relative humidity: 70%

Figure 3-3 gives the resultant predicted temperature changes using DRIFT and HF-Mixture. The flashing model in both DRIFT and HF-Mixture assumes an isentropic (constant enthalpy) flash from the release conditions to atmospheric pressure. The DRIFT predictions are almost identical to the HF-Mixture predictions, giving confidence that the DRIFT thermodynamic model is correctly coded and that the validation of HF-Mixture against experimental data in [12] applies also to DRIFT³.

³ Of course this validation is still limited to the conditions of the experiments, in particular the experimental conditions were such that no condensation liquid of iso-butane is predicted.

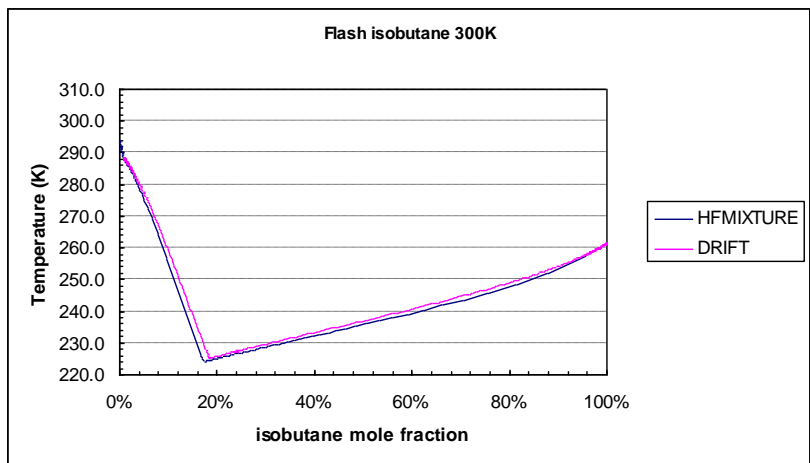
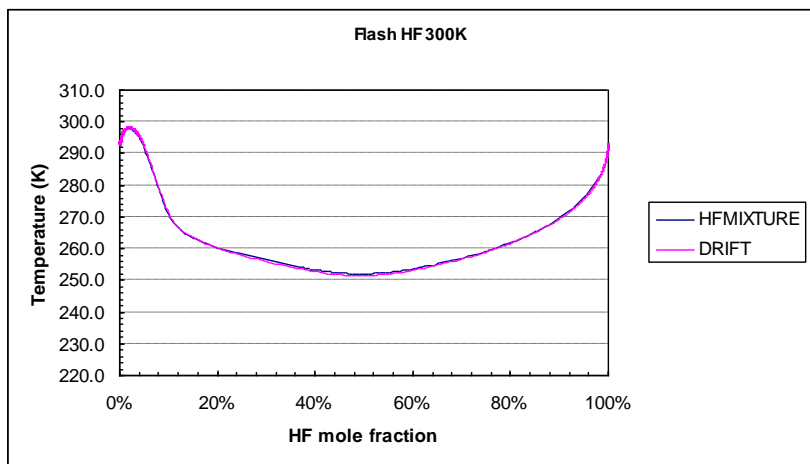
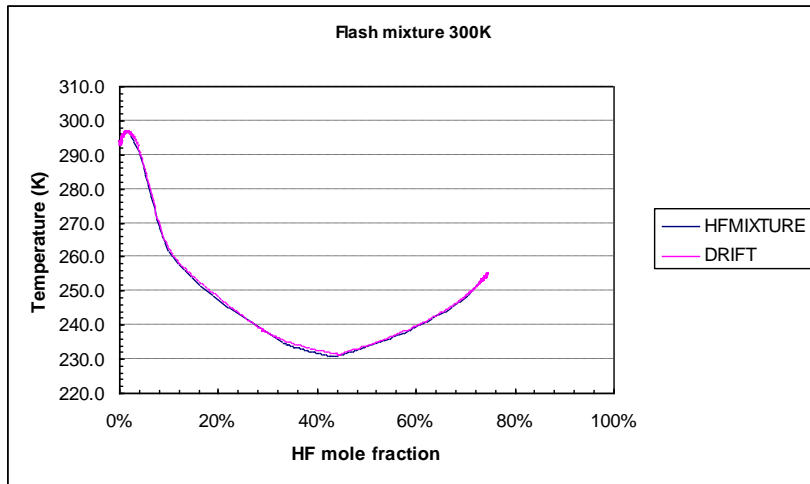


Figure 3-3 Temperature changes resulting from mixing of flashing HF and iso-butane with moist air. Release conditions as in text.

4 HF FIELD TRIAL COMPARISONS

The URAHFREP Campaign 2 field trials released anhydrous HF in different atmospheric conditions. Details of the URAHFREP field trials are reported in refs [3, 16, 17 and 18] and comparisons with DRIFT Version 2 are reported in [19]. In this section results of comparisons with DRIFT Version 3.6.1 are presented. These comparisons provide a useful check on the effect of the changes to the DRIFT model between Versions 2 and 3.

4.1 DRIFT PREDICTIONS

The release conditions for the modelling are the same as used in [19]. To match the time averaging of the different concentration measurements DRIFT results for two averaging times are presented:

- Averaging of the duration of the discharge (appropriate for CEA filters)
- Averaging over 1 s (appropriate for other measurements)

Figure 4-1 compares concentration predictions from DRIFT 3.6.1 with field measurements for the field trails HF007, HF009, HF010 and HF012. Of the URAHFREP field trials, only HF012 was under conditions where enhanced buoyancy may affect dispersion. However, even for HF012 these HF buoyancy effects may be masked by convective atmospheric conditions. Also shown on the plots are the previous results obtained using DRIFT Version 2.27. Although slight differences are apparent between the results using the two versions of DRIFT, the results excepting HF012 are broadly in line with each other and generally compare favourably with the experimental data.

Some of experimental data for HF012 shows a significant dip in concentration between 10m and 200m from the release point compared with the DRIFT predictions. DRIFT also shows a dip, but this is much smaller than dip in the data. DRIFT is predicting HF induced buoyant rise, but the effect of this is much less marked than in the experimental data. There is evidence [16] that the observed rise in HF012 is, at least in part, due to atmospheric convection in low wind unstable conditions. The vertical meander model in DRIFT 3 includes the effect of sampling *both* updrafts and downdrafts based on a probability density model for vertical velocity fluctuations – improved comparison of DRIFT with the observed rise may possibly require sampling a single updraft. The rise effect is transient with DRIFT showing good agreement with the far field measurement at 1000m.

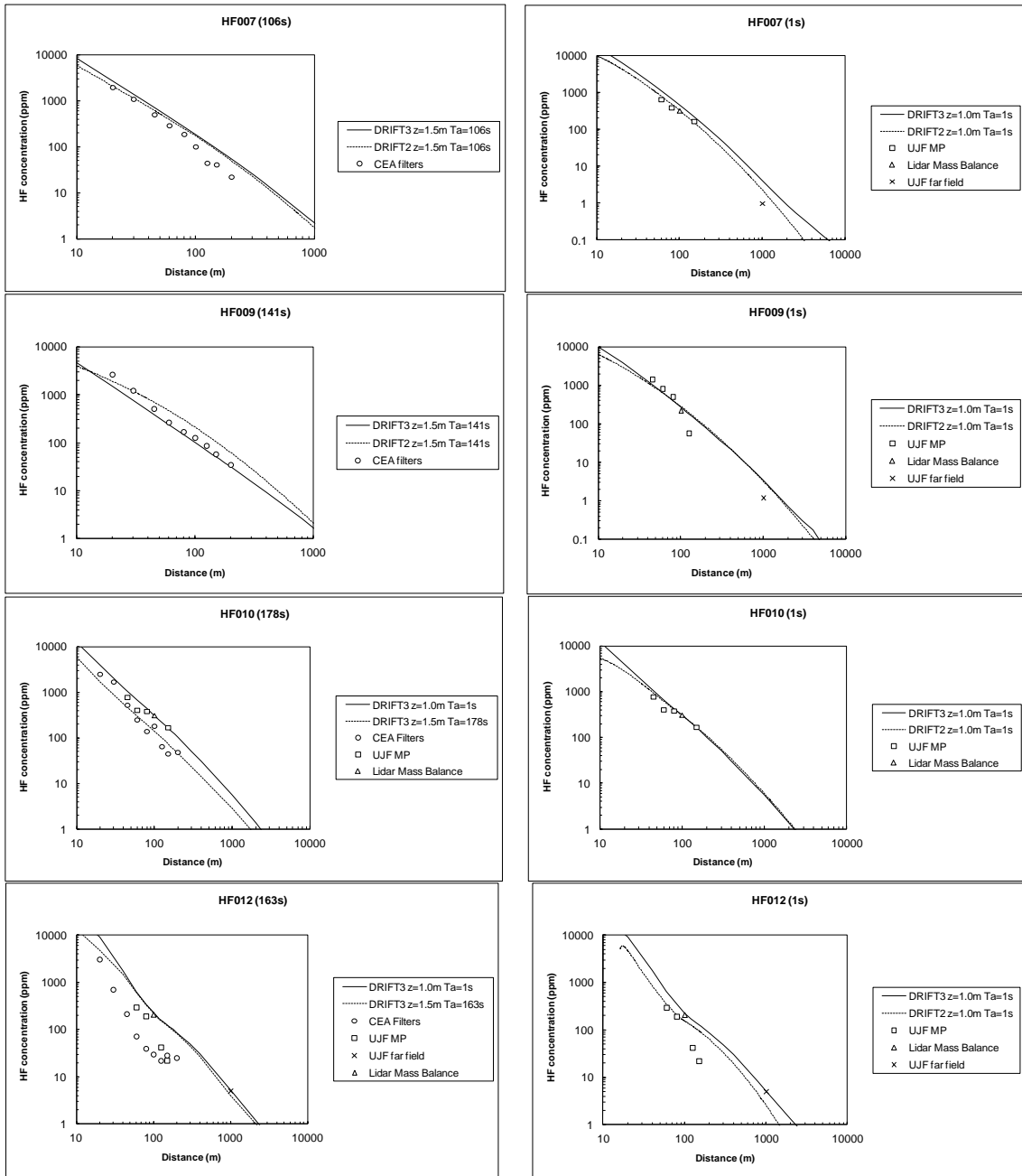


Figure 4-1 Comparison of DRIFT predictions with URAHFREP Campaign 2 concentration measurements

5 SENSITIVITY TO RELATIVE HUMIDITY

In [20] the effects of scaling up the release size and changing the atmospheric stability on plume bulk Richardson number, Ri^* , were studied for a series of superheated liquid HF jets run in EJECT Version 2.10 and, subsequently, in DRIFT Version 2.2.7. Ri^* was used because it is a local measure of buoyancy versus turbulence that is relevant to the lift-off of ground-based buoyant clouds. In the case of HF, Ri^* is predicted to be strongly dependent on relative humidity.

DRIFT Version 2 can only model ground-based clouds: when Ri^* is predicted to become less than a critical lift-off value, the model run terminates. Based upon an analysis of the URAHFREP wind-tunnel data a critical value of -70 was adopted in DRIFT Version 2 as a measure below which ground-level concentrations fall rapidly due to buoyant lift-off. One of the motivations for producing DRIFT Version 3 was to allow the model to run through and beyond this $Ri^* = -70$ critical lift-off point in a smooth manner. DRIFT Version 3 does not directly use Ri^* to determine lift-off, but rather lift-off is calculated as a consequence of the dynamics of the model.

In [20] tables were produced of the minimum values of Ri^* attained and the distance to this minimum value for various release rates, ambient temperatures, Pasquill stability categories, wind speeds and relative humidity. In the case that the $Ri^* = -70$ condition was reached, the minimum Ri^* was reported as “<-70” and the distance to the minimum Ri^* was reported as “>x”, where x is the termination distance. Here we present DRIFT Version 3.6.2 results for a typical case and show the sensitivity of the hazard ranges to relative humidity.

Table 1 in [20] lists the release conditions for all the runs performed. Here we consider just the case of a 1 kg/s release under F2 weather conditions with an ambient temperature of 293 K, the results of which are presented in Table 20 of [20]. Relative humidity values of 40%, 50%, 60%, 70%, 80%, 90% and 100% were studied, and the lift-off criteria was reached in the 90% and 100% cases, with DRIFT Version 2 terminating prematurely at 52m and 45m downstream respectively.

Figures Figure 5-1: Side elevation for 1 kg/s release of HF in F2 weather conditions with ambient temperature of 293 K and relative humidity of 40%. to Figure 5-7: Side elevation for 1 kg/s release of HF in F2 weather conditions with ambient temperature of 293 K and relative humidity of 100%. show side-elevation contours plots produced using DRIFT Version 3 for the relative humidity values given above. The contour shown is to the Dangerous Toxic Load for Specified Level of Toxicity (SLOT DTL) for HF, which is 12,000 ppm.min. The contour plots are shown at unit aspect-ratio.

The cases of 90% relative humidity (Figure 5-6) and 100% relative humidity (Figure 5-7), which both terminated at the critical lift-off Ri^* in DRIFT Version 2, now successfully run past this point in DRIFT Version 3. Notice that the cloud centreline is predicted to start to lift-off from the ground at a distance approximately corresponding to the critical lift-off Ri^* value. This correspondence of lift-off point is reassuring since DRIFT Version 3 does not use a critical lift-off parameter approach for determining the onset of lift-off.

The results indicate that buoyant lift-off due to HF-water interactions in humid conditions has the potential to considerably shorten the hazard range compared with lower humidity conditions. For the particular example cases considered, this effect gives approximately an order of magnitude difference in hazard range between the 50% relative humidity case and the 100% relative humidity case. An exception to this trend is the 40% relative humidity case which has a slightly shorter hazard range than the 50% case - this is due to the dense ground-based cloud being wider in 40% humidity as a result of enhanced lateral (gravity) spread.

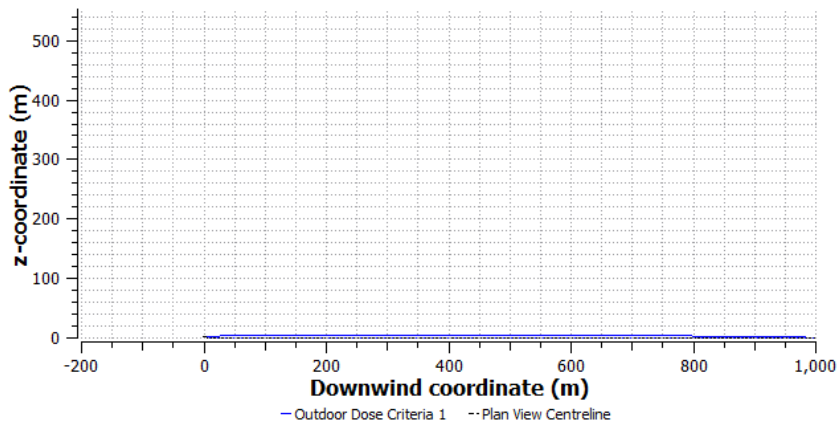


Figure 5-1: Side elevation for 1 kg/s release of HF in F2 weather conditions with ambient temperature of 293 K and relative humidity of 40%.

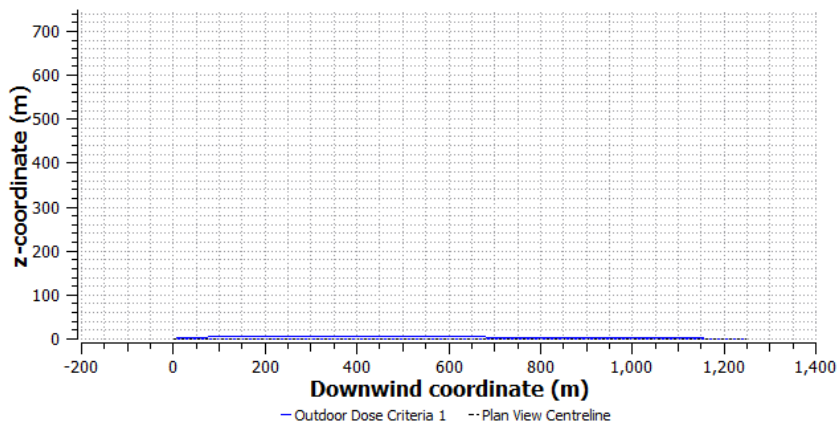


Figure 5-2: Side elevation for 1 kg/s release of HF in F2 weather conditions with ambient temperature of 293 K and relative humidity of 50%.

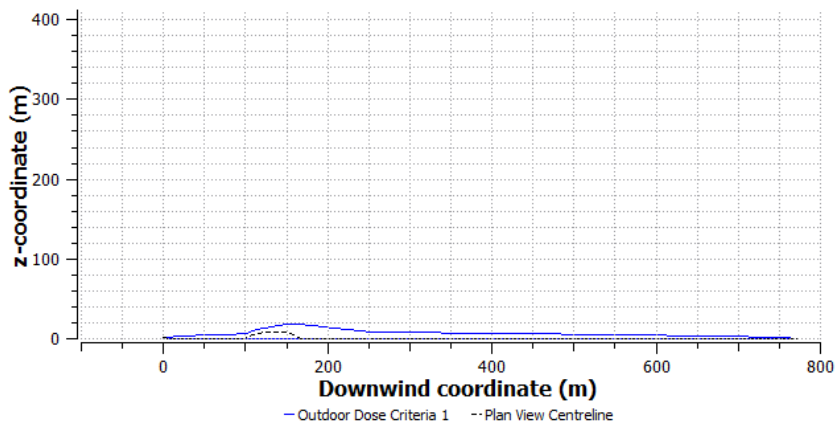


Figure 5-3: Side elevation for 1 kg/s release of HF in F2 weather conditions with ambient temperature of 293 K and relative humidity of 60%.

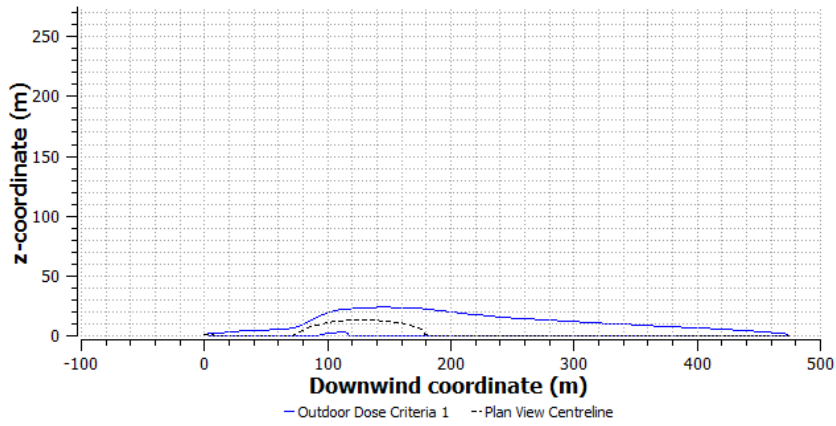


Figure 5-4: Side elevation for 1 kg/s release of HF in F2 weather conditions with ambient temperature of 293 K and relative humidity of 70%.

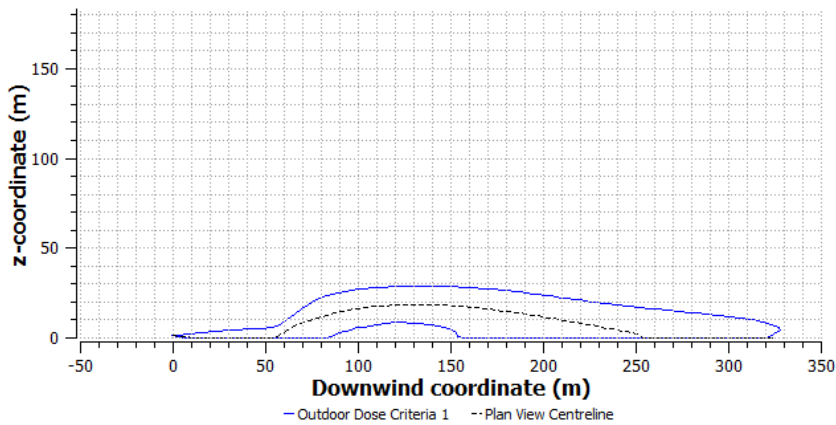


Figure 5-5: Side elevation for 1 kg/s release of HF in F2 weather conditions with ambient temperature of 293 K and relative humidity of 80%.

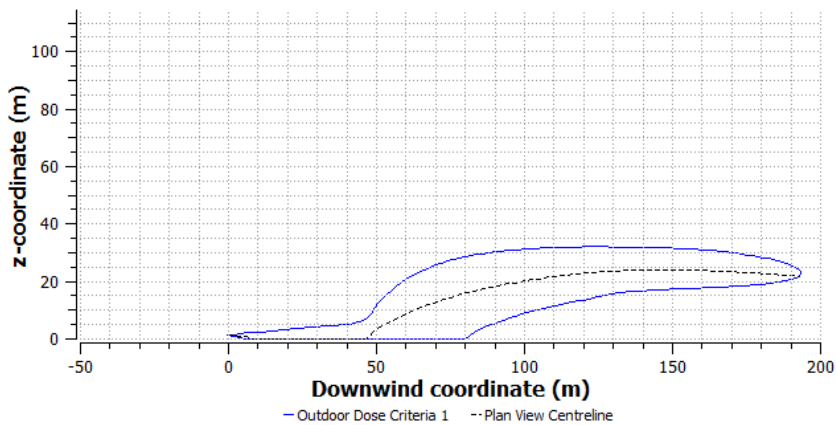


Figure 5-6: Side elevation for 1 kg/s release of HF in F2 weather conditions with ambient temperature of 293 K and relative humidity of 90%.

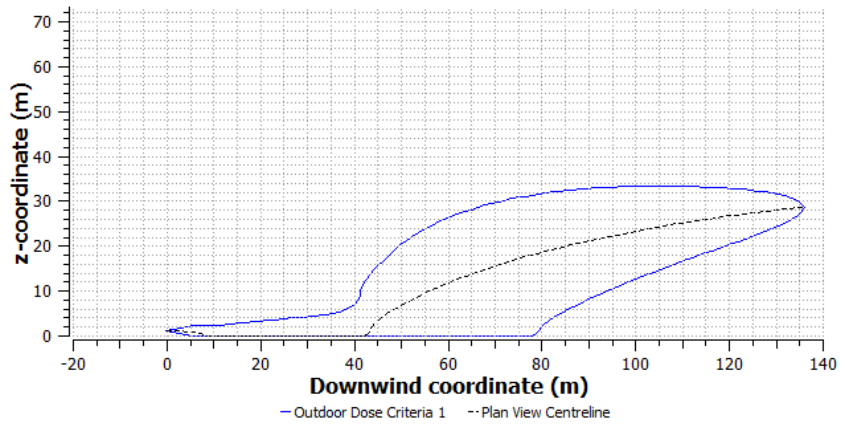


Figure 5-7: Side elevation for 1 kg/s release of HF in F2 weather conditions with ambient temperature of 293 K and relative humidity of 100%.

6 CONCLUSIONS

6.1 COMPARISONS WITH WIND-TUNNEL DATA

Comparisons of DRIFT predictions with wind-tunnel data for ground level buoyant sources indicate:

- The effect of buoyancy on maximum centreline concentration is well represented
- The buoyancy at which the transition occurs from ground-based plume to elevated plume is well represented, even for the widest source, which was found not be well represented by the same ‘critical lift-off parameter’ as less wide sources, or by simple models in previous studies. An exception is the longest ‘Long Source’, which shows more rapid lift-off in the wind-tunnel than predicted by DRIFT. This is possibly a result of lift-off occurring over the source which is not well represented by DRIFT’s bulk treatment of the plume cross-section.
- The predicted rise of the location of maximum buoyancy is in reasonable agreement with the wind-tunnel data, albeit with a slight tendency to under-predict plume rise. When ‘added mass’ was included within the DRIFT model equations, insufficient plume rise is predicted.
- For the cases where the plume has lifted-off from the ground, the ground-level concentrations predicted by DRIFT are larger than observed in the experimental measurements. This may, in part, be related to the assumed shape of the elevated plume being axi-symmetric whereas a very buoyant plume may become ‘kidney’ shaped.

The wind-tunnel data, and DRIFT model predictions, for buoyant puff releases are much more variable. Comparisons of DRIFT predictions with the data indicate:

- The effect of buoyancy on maximum centreline concentration is, in general, well represented and reflects the expected trends – in particular buoyant puffs show more rapid dilution and less buoyant rise than buoyant plumes with the same buoyancy flux.
- Modelling the releases as either finite duration or instantaneous generally produces similar maximum concentration predictions, indicating that the releases are best scaled with total buoyancy, rather than buoyancy flux. However, the DRIFT modelling does show differences in lift-off height between the finite duration and instantaneous models, with the lift-off height from the instantaneous model being in better agreement with the experimental data.
- The model predictions for puff releases are with ‘added mass’ included as in the model of Turner on which DRIFT’s buoyant puff model is based.

The asymptotic behaviour of DRIFT predictions for lift-off of buoyant puffs in low wind agree well with an analytic solution [11] to the model of Turner. This provides a useful verification check.

6.2 COMPARISONS WITH HF THERMOYNAMICS DATA

- Comparisons with the HF-moist air mixing data of Schotte and with HF-moist air mixing data from URAHFREP indicate that the Drift Version 3 thermodynamic model implementation agrees with earlier model implementations (including DRIFT Version 2 and the URAFHREP model HF-Mixture).
- Comparisons indicate that the predictions for HF-iso-butane mixtures with moist air from DRIFT Version 3 are almost identical to those from HF-Mixture. This is a useful verification check, and also is indirect validation, since good agreement between HF-

Mixture and URAHFREP experimental data was observed for HF-iso-butane mixtures in [12].

6.3 COMPARISONS WITH FIELD TRIALS DATA

Comparisons with URAFHREP field trial data indicate that:

- DRIFT Version 3 performs similarly to DRIFT Version 2, noting that in only one of the field trials (HF012) were conditions such that HF induced buoyant rise may affect dispersion, and that this may be masked by atmospheric convection.
- Despite the use of different averaging time models in DRIFT Version 3 [2] and DRIFT Version 2 [19], the predicted effect of time averaging is similar and in approximate accord with the field data.

6.4 SENSITIVITY TO RELATIVE HUMIDITY

Example runs for 1 kg/s HF releases indicate:

- The ability of DRIFT Version 3 to run through the transition between ground-based and elevated clouds enables hazard ranges to be obtained for a much wider set of conditions than was possible using DRIFT Version 2.
- The sensitivity of HF concentration to relative humidity and illustrate the need for care when choosing the representative values for use in risk assessment.

6.5 CONCLUDING REMARKS

This study indicates that the buoyant enhancements incorporated into DRIFT Version 3 perform reasonably well compared with experimental data. The influence of buoyancy on maximum concentration appears to be well represented. The prediction of other parameters, e.g. buoyant plume and puff rise is more variable, but appears reasonable overall. Ground-level concentration predictions for lifted-off plumes are too large compared with wind-tunnel measurements. It is difficult to adjust the model to improve this aspect without having a detrimental impact on the other predictions which compare well. Further work on this might be beneficial. However, we caution against too closely tuning the model to a particular dataset without having an independent data set against which to validate this. Indeed, it is comforting that the reasonably good overall agreement found in this study is without any adjustment of DRIFT model parameters (apart from the neglect of ‘added mass’ for the buoyant plume model). Our comparisons of the buoyant wind-tunnel data with DRIFT predictions may also lend indirect support to other integral dispersion models which model buoyant lift-off and dispersion in a similar way to DRIFT.

Comparison with experimental data indicates that the thermodynamic behaviour of mixtures of hydrogen fluoride with moist air is well established. Extending models to include other components, e.g. iso-butane is less certain, although URAHFREP measurements support iso-butane acting as a diluent which may counteract buoyancy generation. The DRIFT Version 3 comparisons reported here simply verify that the new coding of the model agrees with earlier implementations.

The comparisons with URAHFREP field trials data show that both DRIFT Version 3 and DRIFT Version 2 can adequately represent these real HF releases. However, using DRIFT Version 3, much larger HF releases than in the URAHFREP field trials can now be modelled in humid, low-wind conditions – the results from which depend on DRIFT’s buoyant lift-off model, which is shown here to be in reasonably good agreement with wind-tunnel data. The sensitivity of model predictions to atmospheric humidity should be considered when selecting representative scenarios for risk assessment involving releases of anhydrous HF.

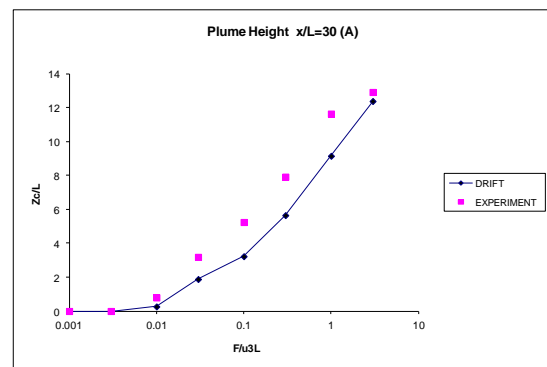
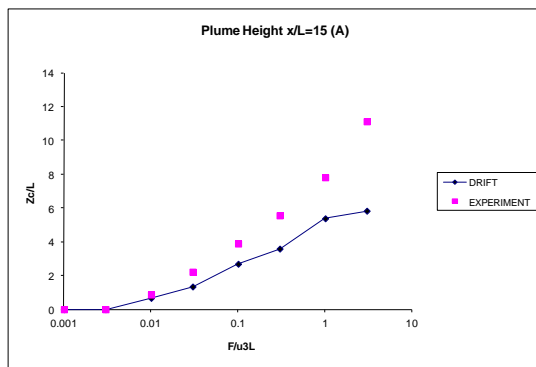
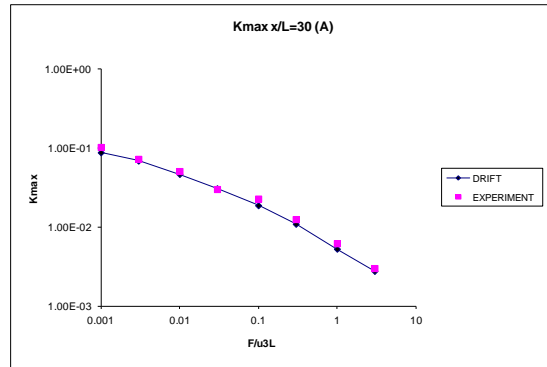
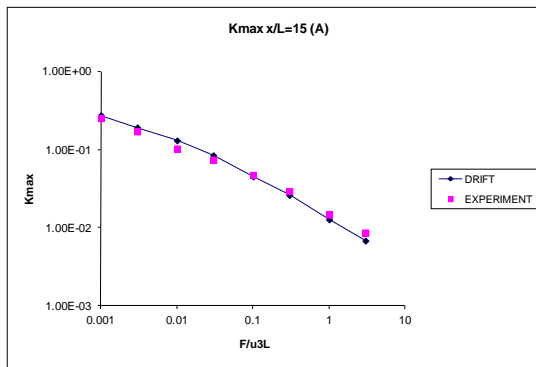
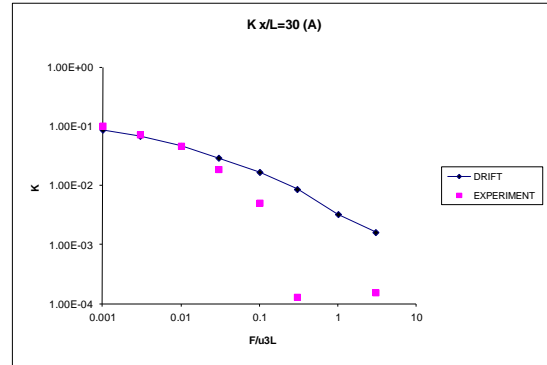
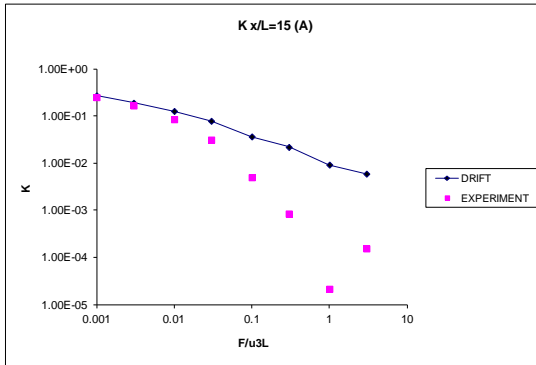
7 REFERENCES

1. Tickle, G. A. and Carlisle J. E (2008), “Extension of the Dense Gas Dispersion Model DRIFT to Include Buoyant Lift-off and Rise”, HSE Research Report RR629.
2. Tickle G. A. and Carlisle J. E. (2011), “DRIFT Version 3 Mathematical Model”.
3. Porter S. and Nussey C. (2001), “A Summary of the URAHFREP Project”, URAHFREP: PL97115, EU Contract ENV4-CT97-0630.
4. Tickle G. A. (2011), “Comparisons of DRIFT Version 3 Predictions with DRIFT Version 2 and Experimental Data”, ESR Technology Report ESR/D1000846/STR01/ Issue 1.
5. Tickle, G. A. (2001), Integral Modelling of the Dilution and Lift-off of Ground Based Buoyant Plumes and Comparison with Wind Tunnel Data, AEA Technology Report, AEAT/NOIL/27328006/001(R) Issue 1.
6. Hall, D. J. & Walker, S. (2000), “Plume Rise from Buoyant Area Sources at the Ground”, BRE Report No. 80921.
7. Hall, D.J., Walker, S., and Tily, P.J. (2001), “Puff Rise from Buoyant Area Sources at the Ground”, BRE Report No. 202614.
8. Nielsen M and Ott S (1995,) “A Collection of Data from Dense Gas Experiments”, Risø Laboratory Report Risø-R-845(EN), ISBN 87-550-2113-1
9. Walton, E. (2011), “DRIFT COM Interface Guide”, ESR Technology, Project No. D1000846.
10. Turner J. S. (1973), Buoyancy Effects in Fluids, Cambridge University Press, ISBN 0 521 08623 x.
11. Fannelöp, T. K. (1994), Fluid Mechanics for Industrial Safety and Environmental Protection, Industrial Safety Studies, Elsevier, ISBN: 0-444-89863-8.
12. Tickle, G. A. (2001), Thermodynamic Modelling of Anhydrous HF/Moist Air/Immiscible Component Mixtures and Validation Against Experimental Data, AEA Technology Report, AEAT/NOIL/27328006/002(R) Issue 2.
13. Clough P. N., Grist D. R. and Wheatley C. J. (1987), “Thermodynamics of Mixing and Final State of a Mixture formed by the Dilution of Anhydrous Hydrogen Fluoride with Moist Air”, UKAEA Report SRD/HSE/R 396, 1987
14. Schotte W. (1987), “Fog Formation of Hydrogen Fluoride in Air”, Ind. Eng. Chem. Res. 1987, Vol 26, pp300-306
15. Kemp C. K. and Newland M. S. (2000), “HF Thermodynamic Tests: Data Report”, AEA Technology Report AEAT/R/NS/0028, January 2000.
16. Ott S. and Jørgensen H. E. (2001) ,“Meteorology and lidar data from the URAHFREP field trials”, Risø Report Risø-R-121(EN)
17. Bettis R. J. and Allen J. T. (2001), “URAHFREP Field Campaign 2 (August 2000) Results from the Health and Safety Laboratory Plume Measurements”, HSL Report FR/01/02B
18. Trégoures A., Saint-Bonnet P., Chenevier M. and Romanini D. (2001), “URAHFREP Work Package 2 – Concentration Measurements”, CEA Report DTEN/DR/2001/24/AT/CR In. 0.
19. Tickle G. A. (2001), “Model Predictions Compared with URAHFREP Campaign 2 Field Trial Data”, AEA Technology Report, AEAT/NOIL/27328006/002(R) Issue 2.
20. Tickle G. A. (2001), “Humidity and Windspeed Dependence of Model Predictions for Richardson Number Lift-Off Parameter”, AEA Technology Report, AEAT/NOIL/RD03637002/001(R)

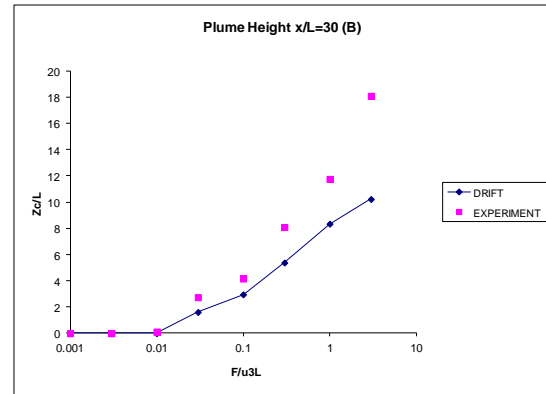
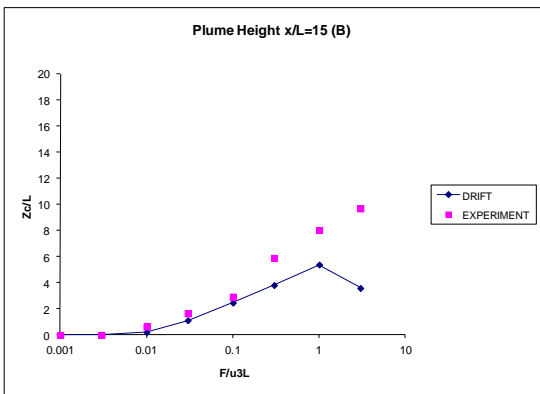
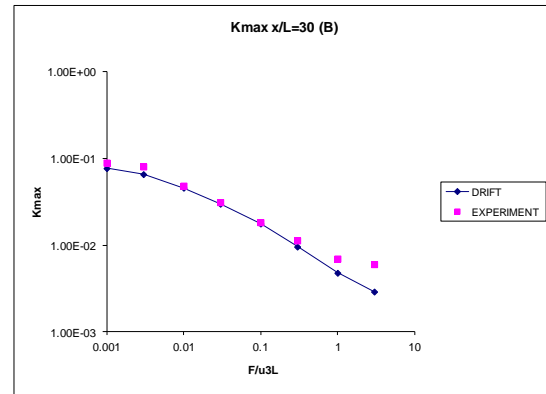
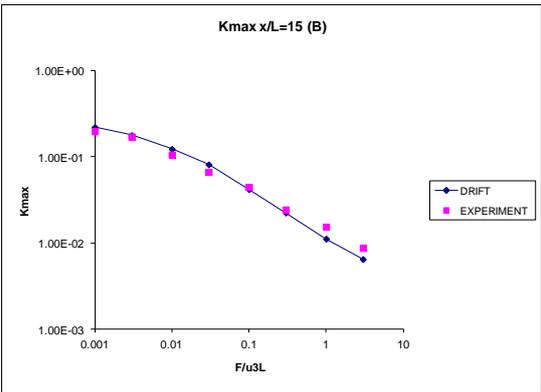
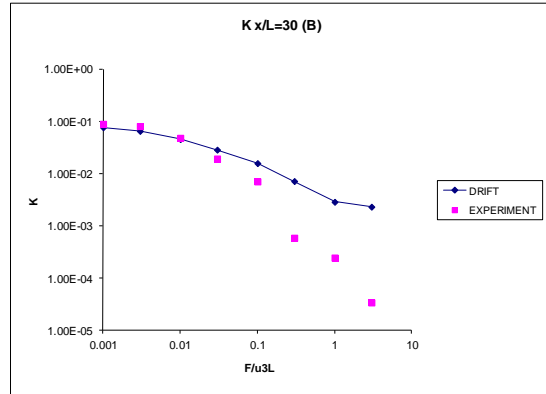
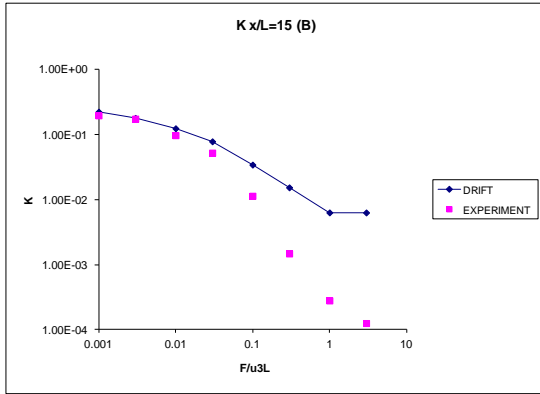
APPENDICES

APPENDIX 1 BUOYANT PLUME GRAPHS

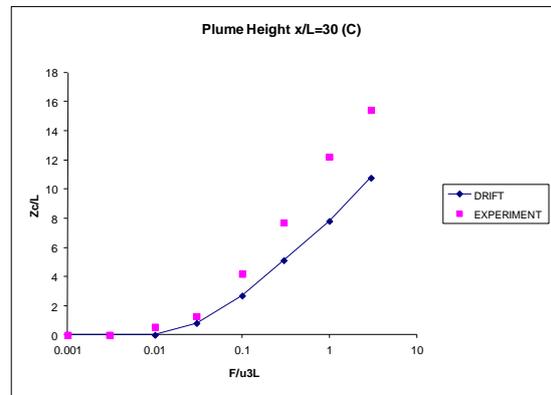
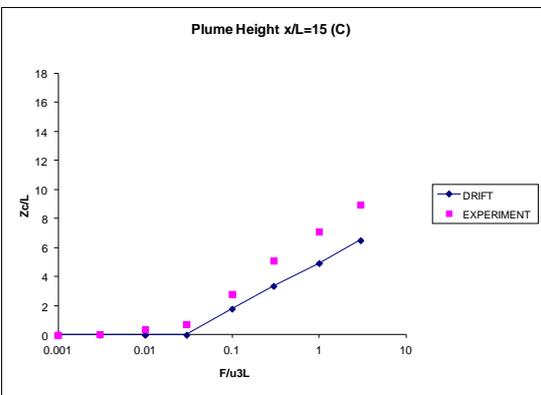
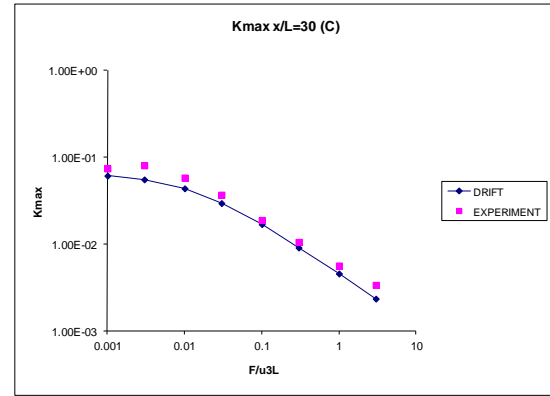
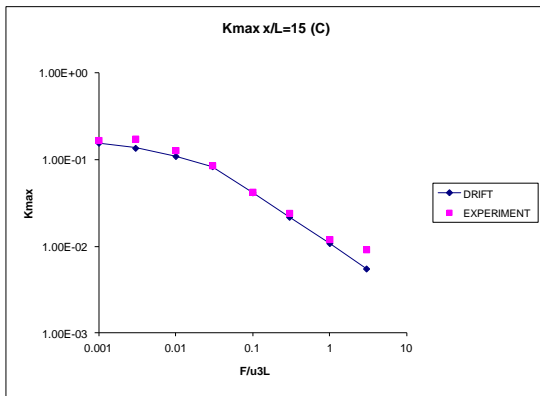
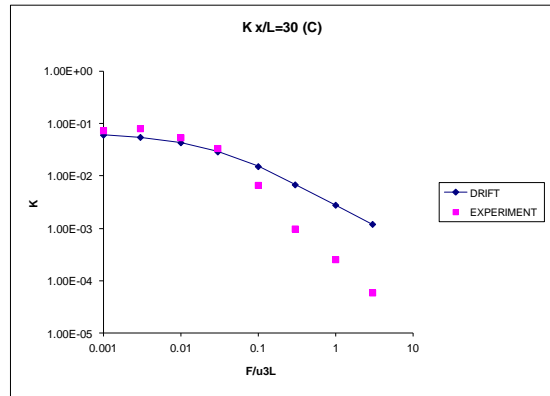
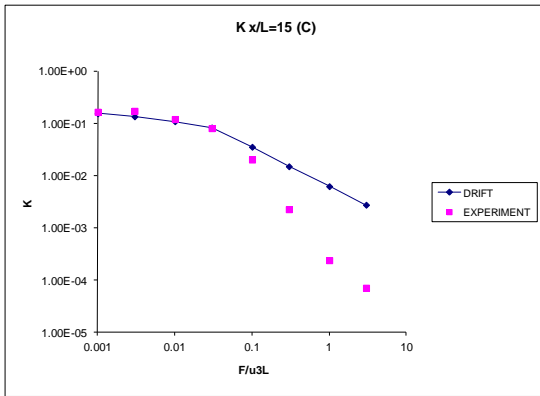
Source A



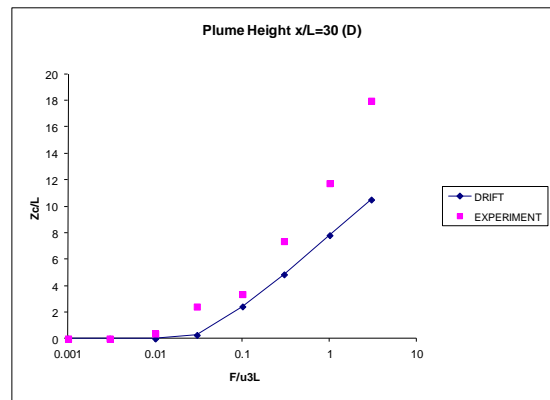
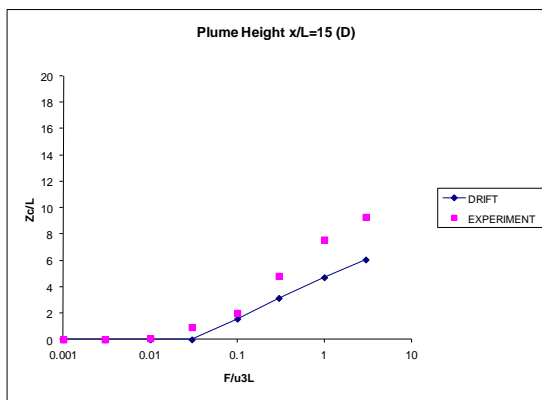
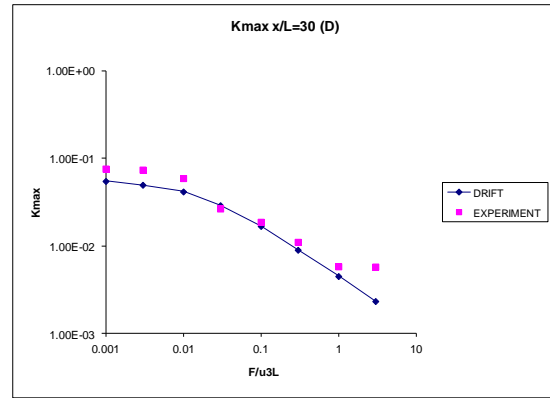
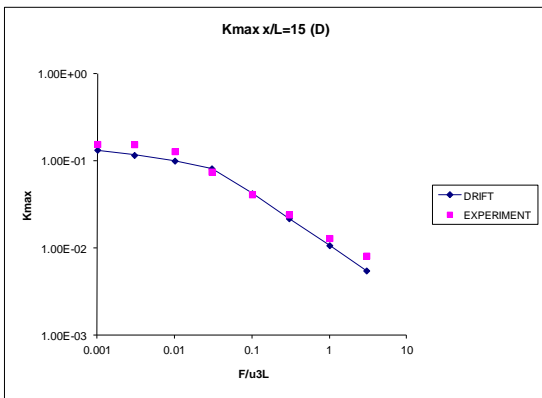
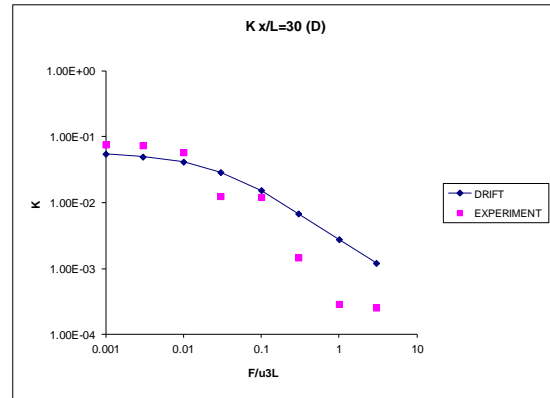
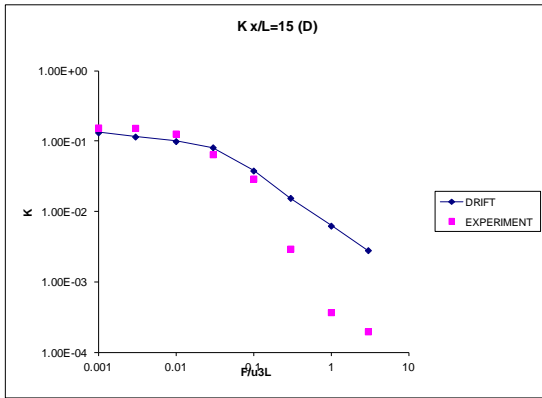
Source B



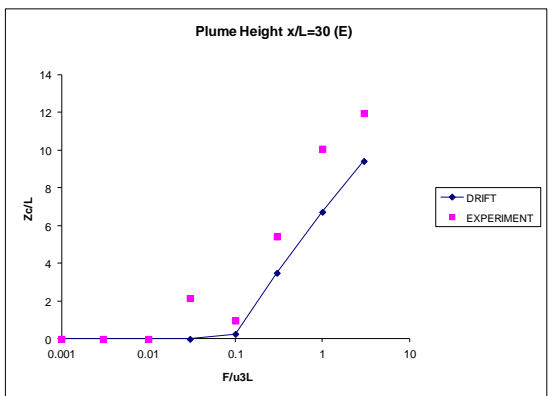
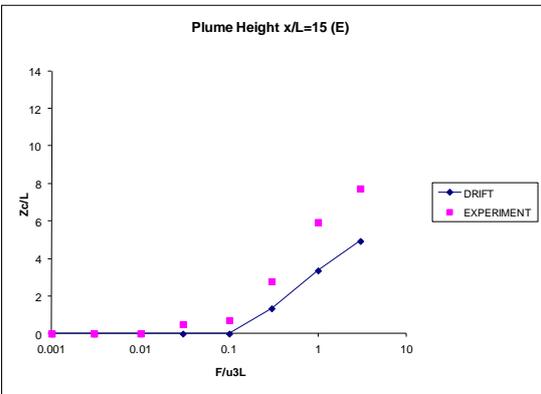
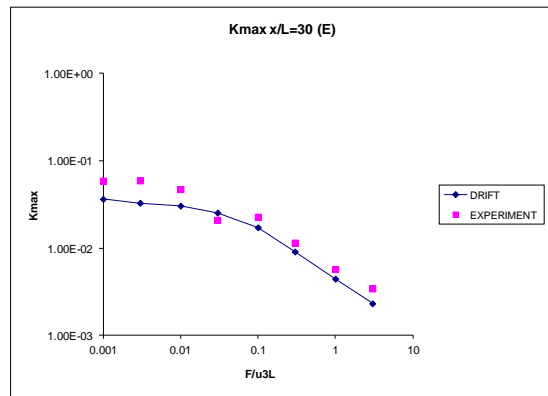
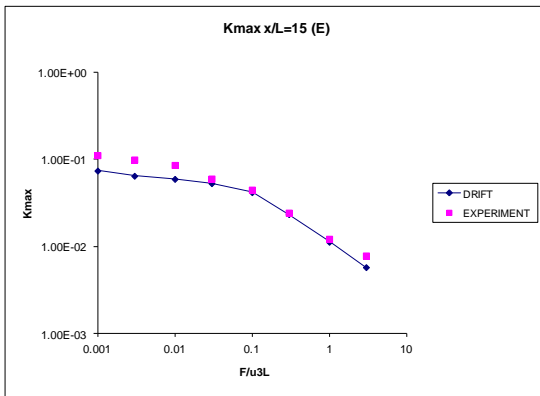
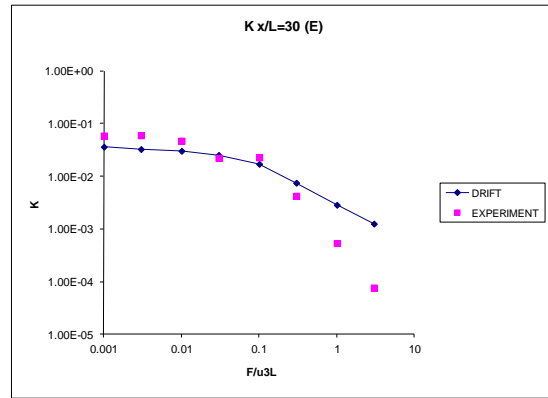
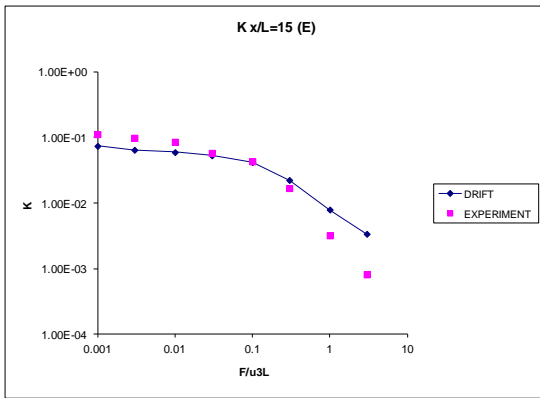
Source C



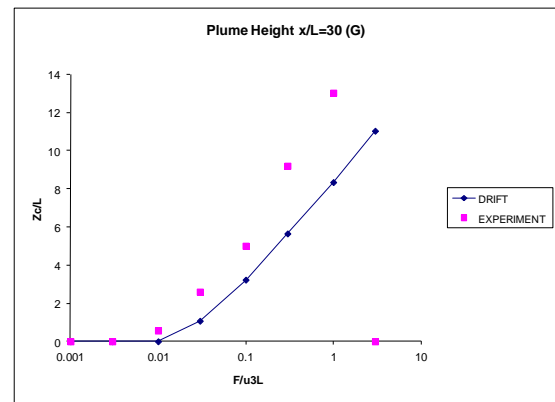
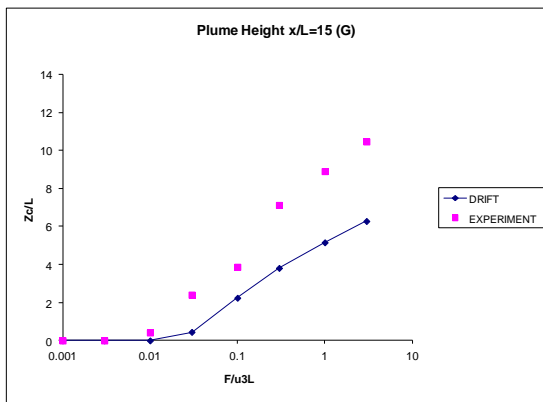
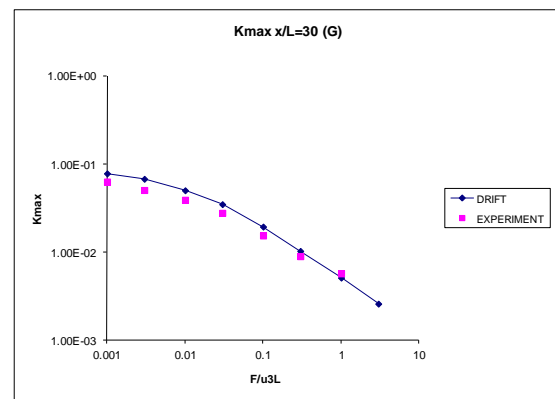
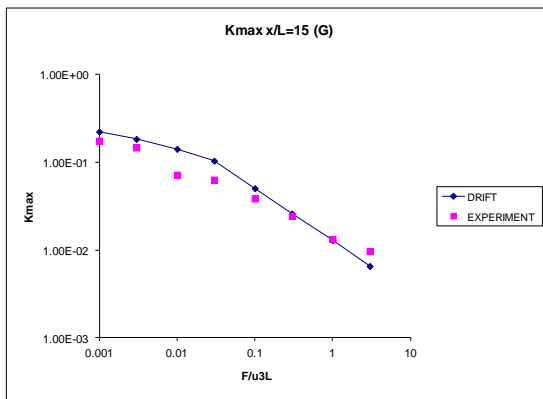
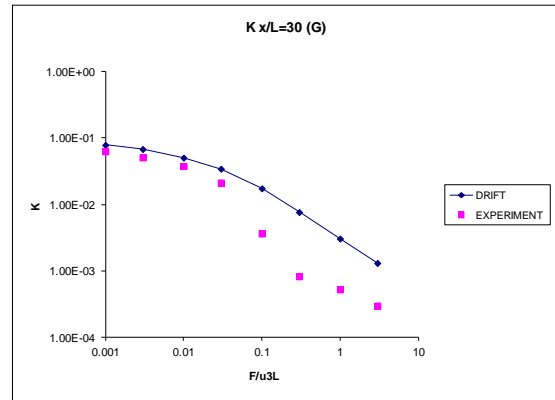
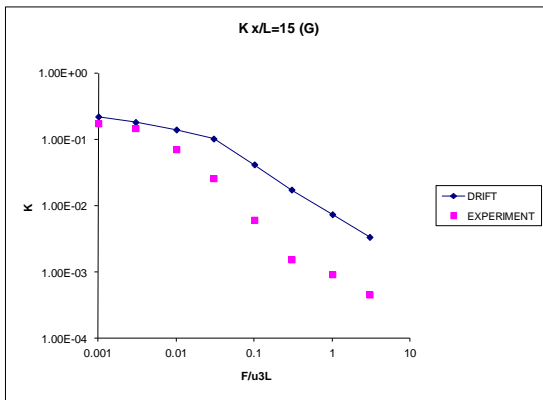
Source D



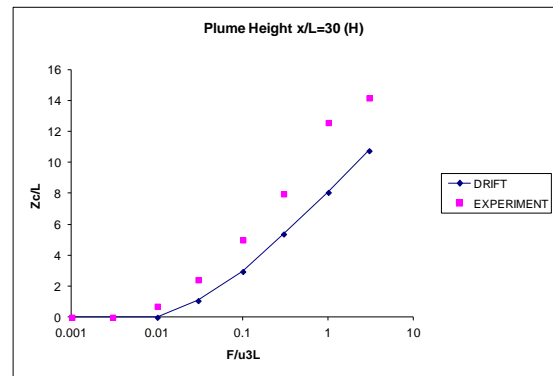
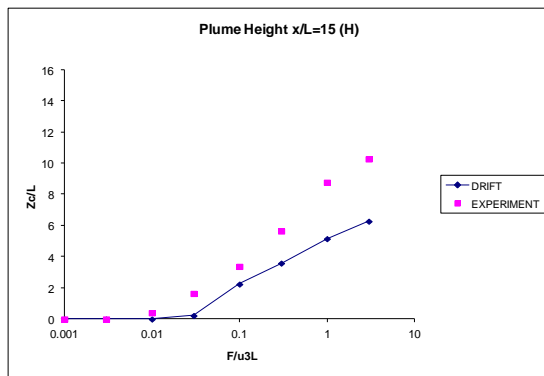
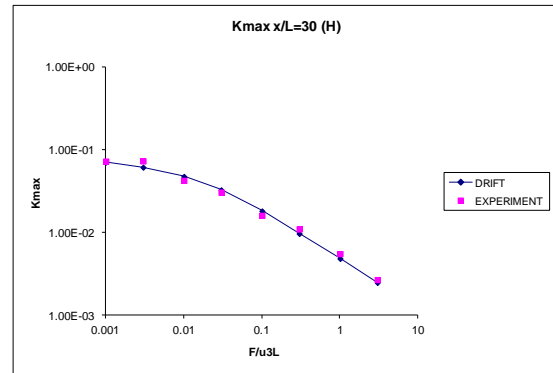
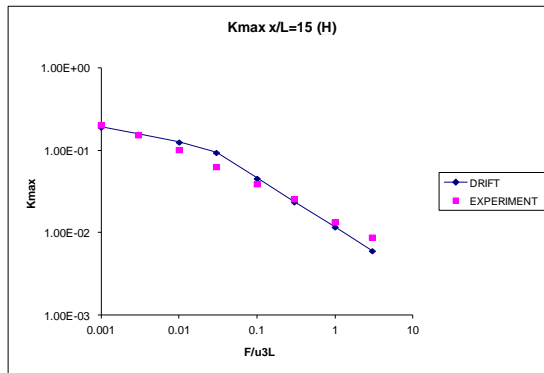
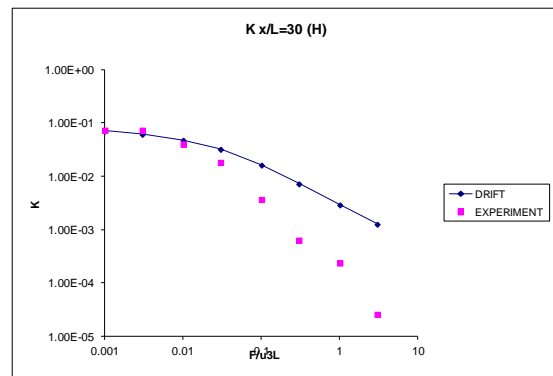
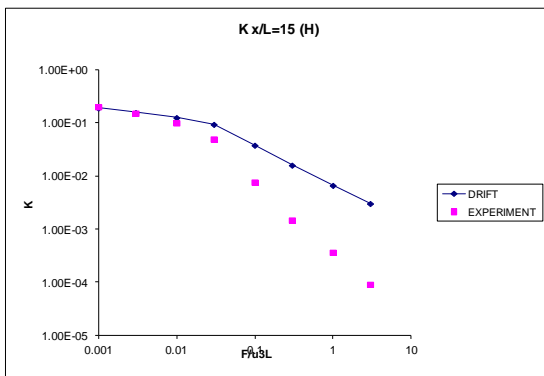
Source E



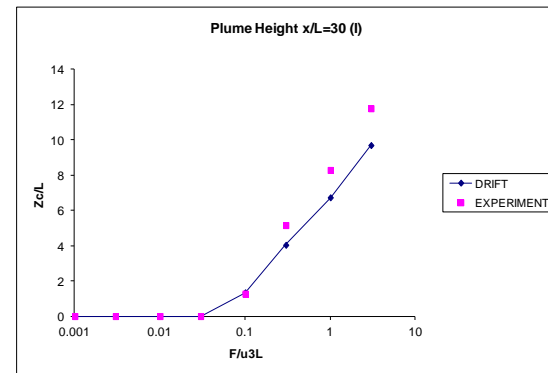
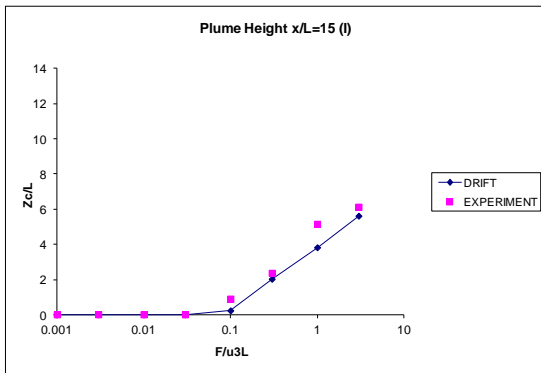
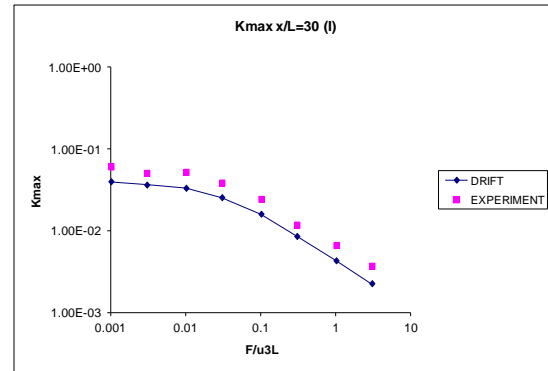
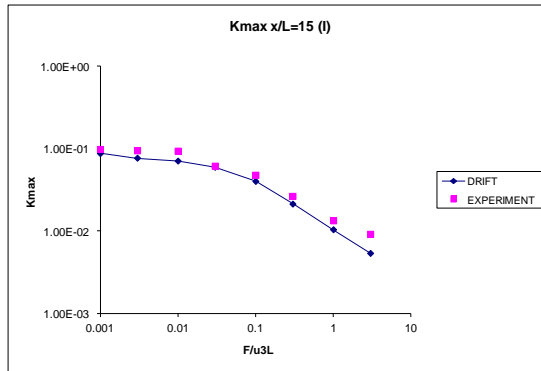
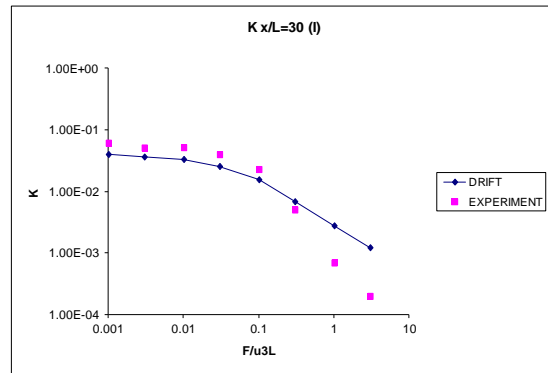
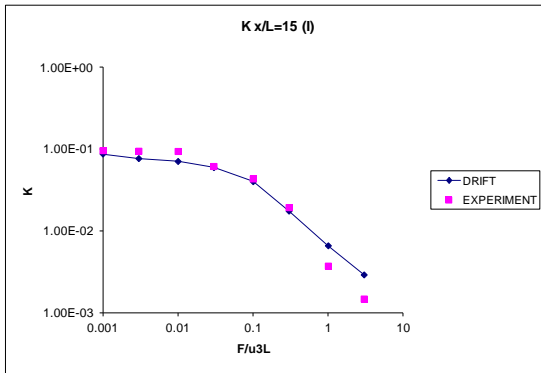
Source G



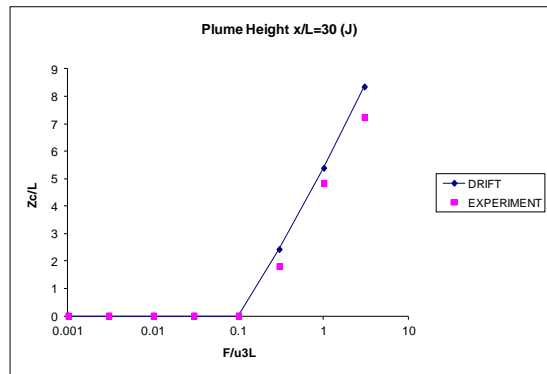
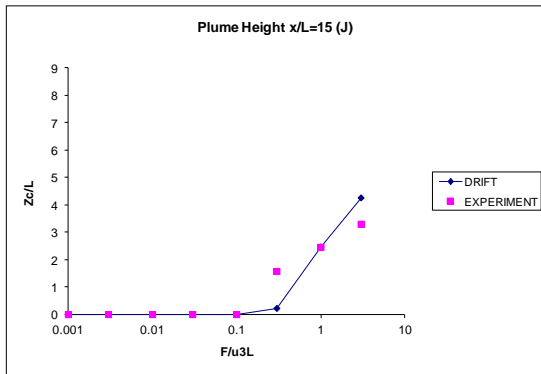
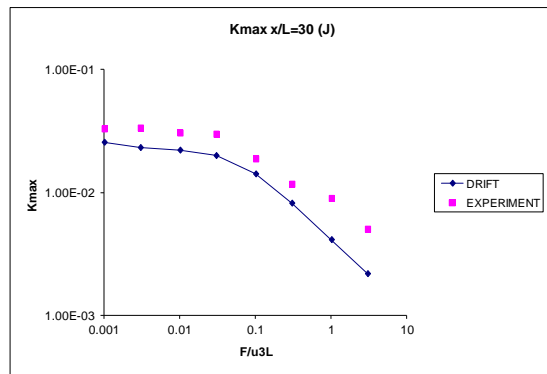
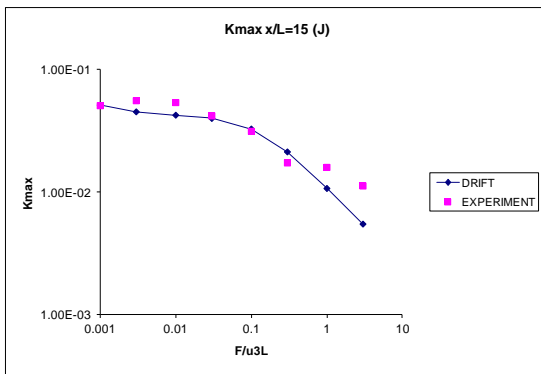
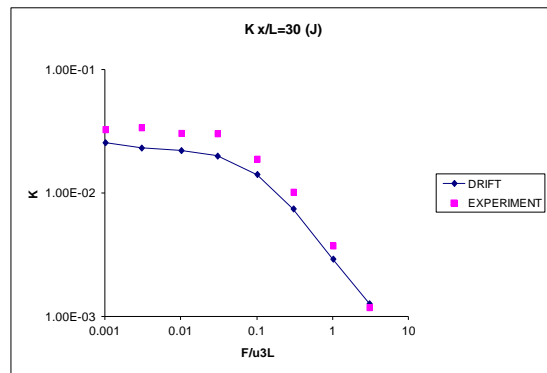
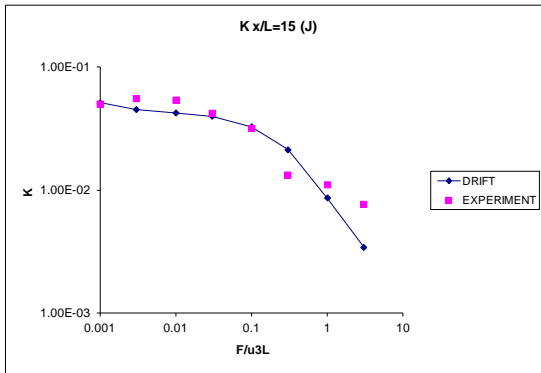
Source H



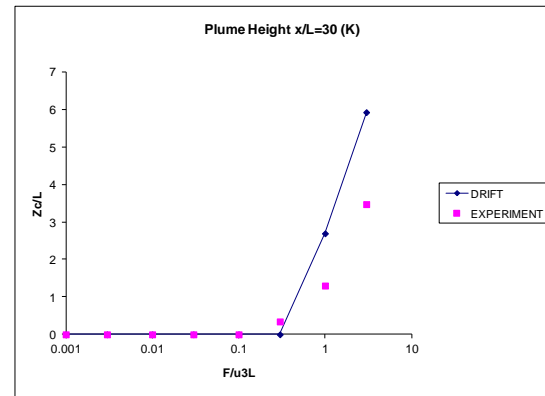
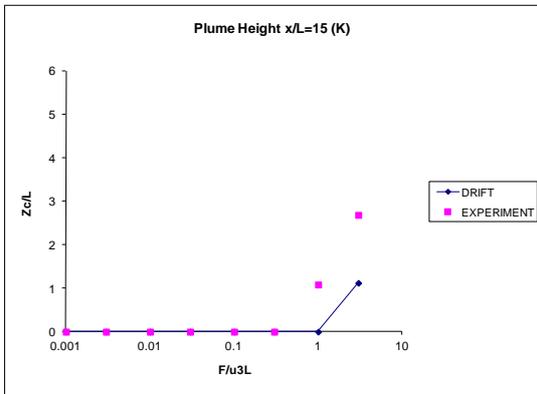
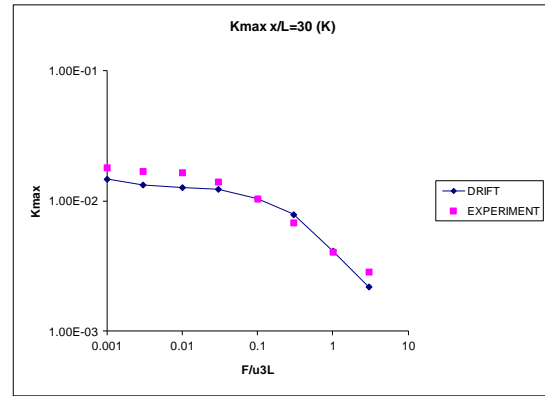
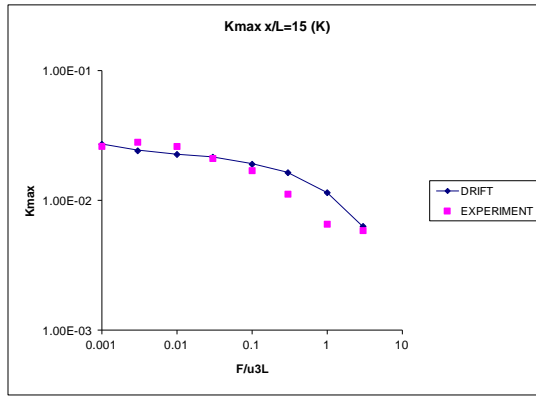
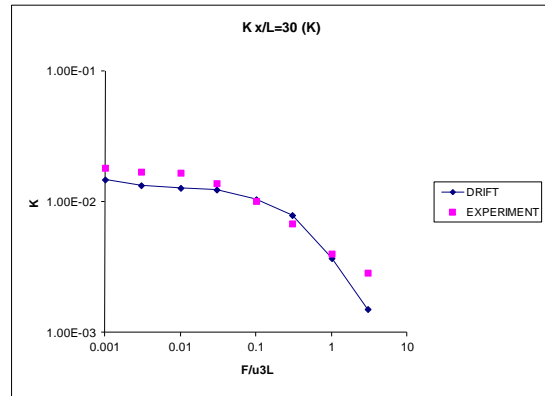
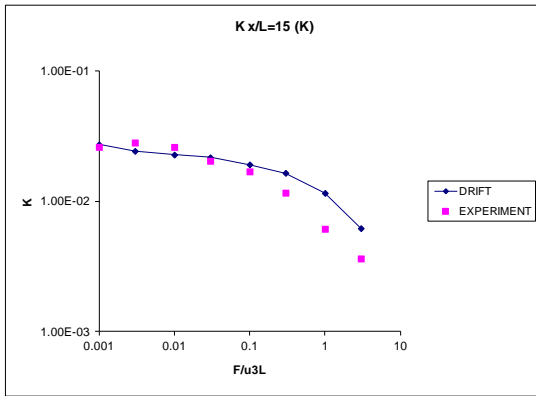
Source I



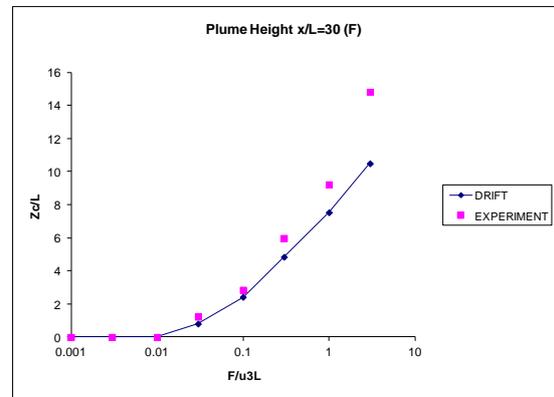
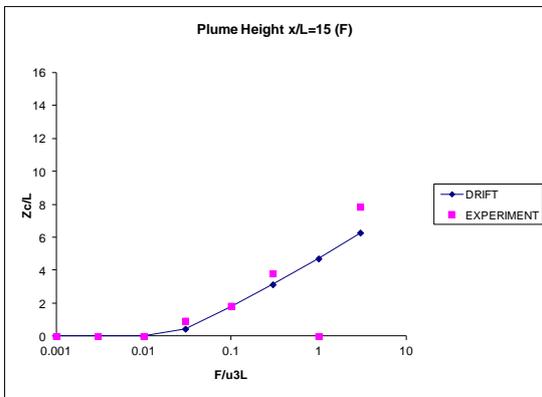
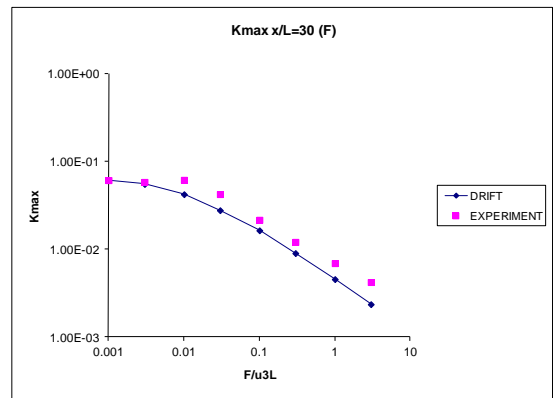
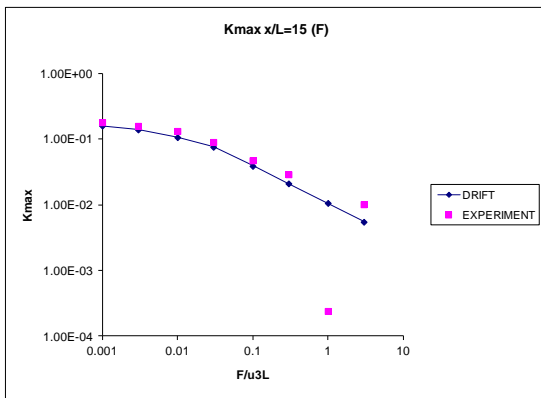
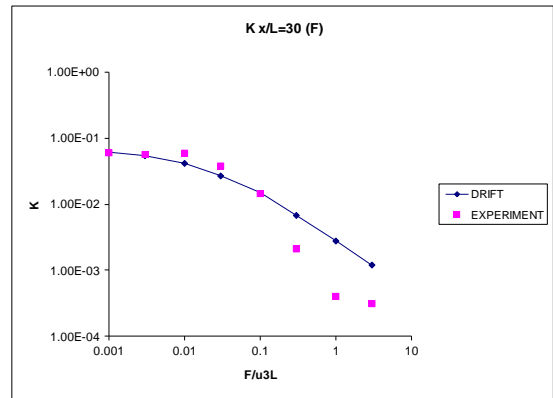
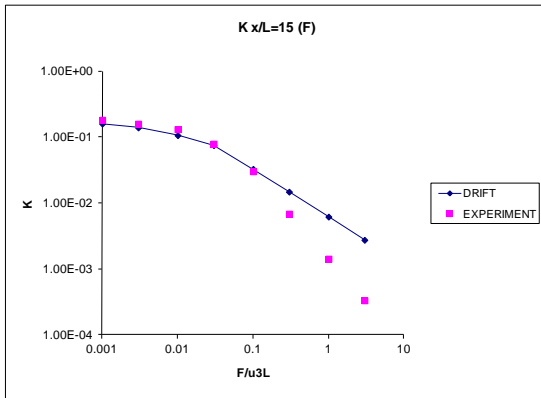
Source J



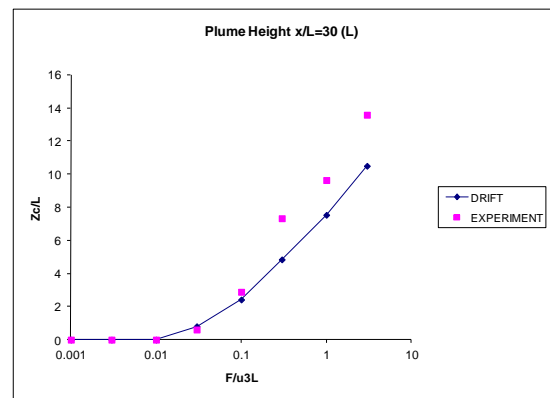
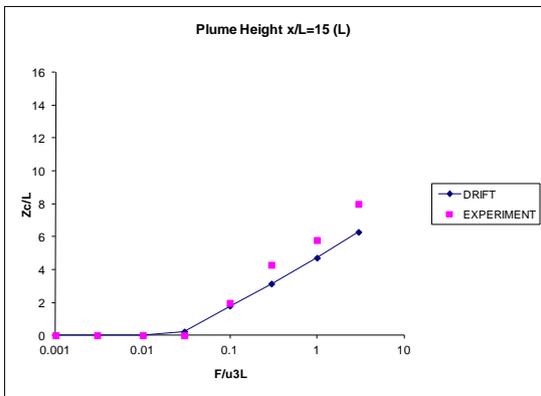
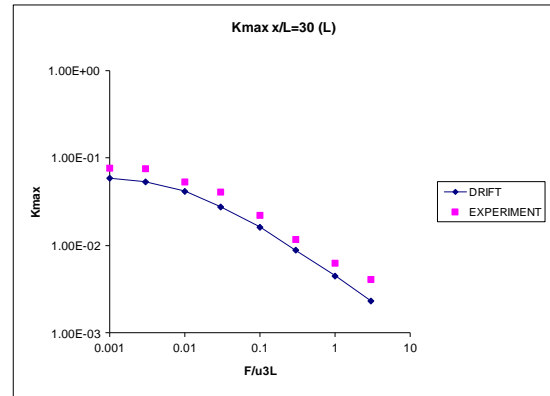
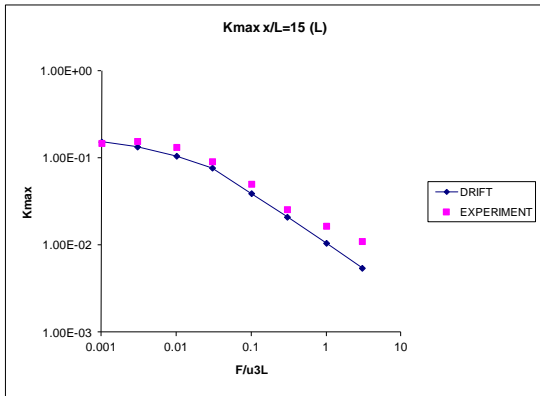
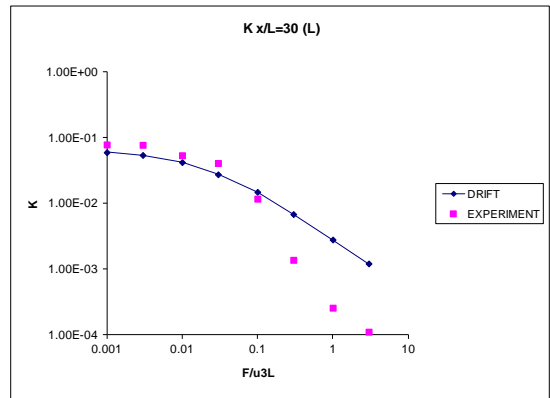
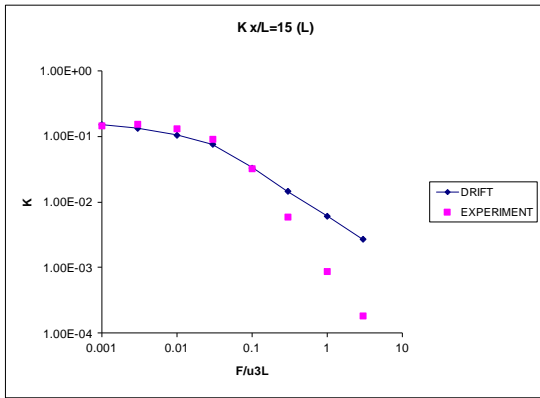
Source K



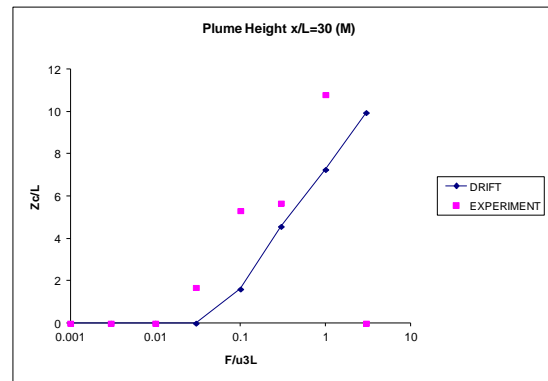
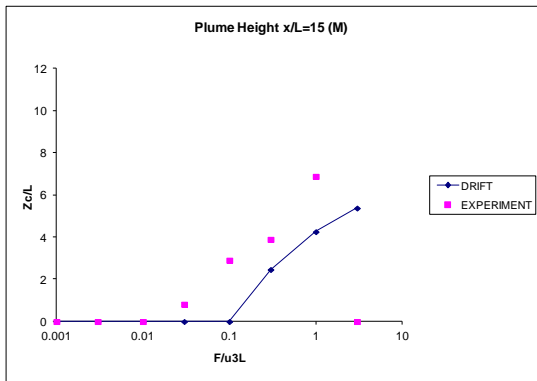
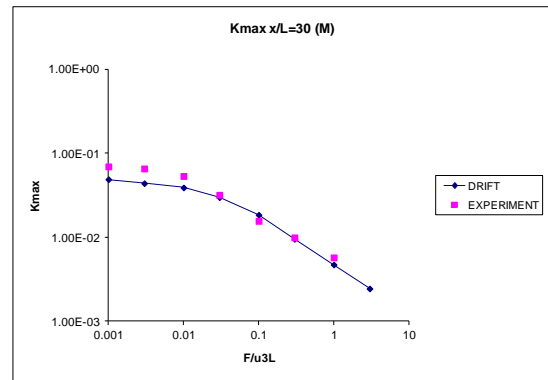
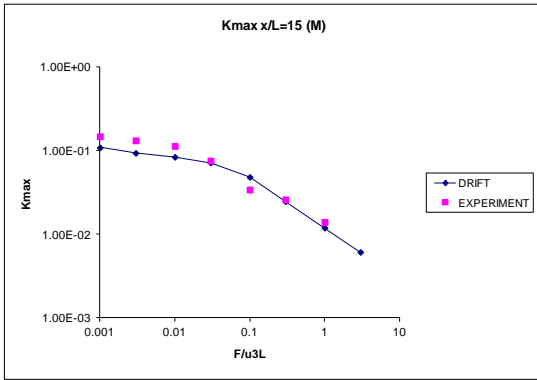
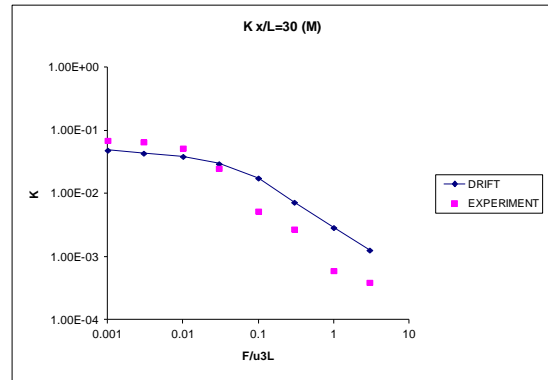
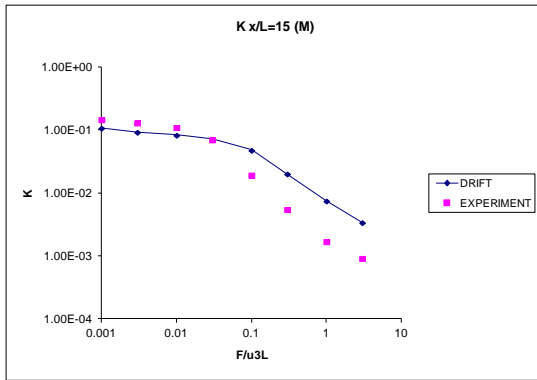
Source F



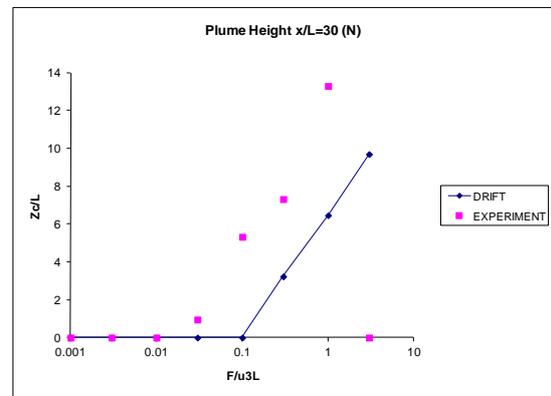
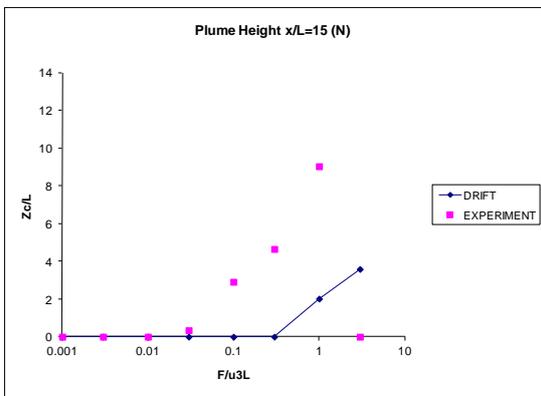
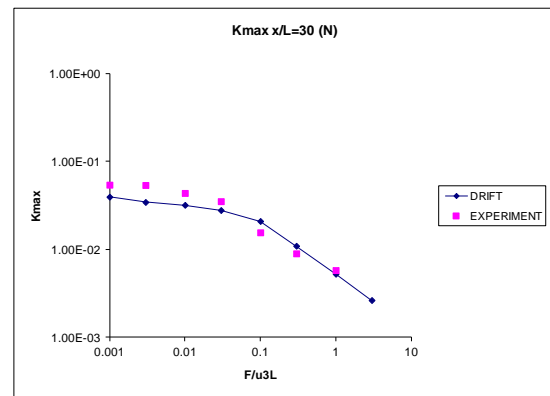
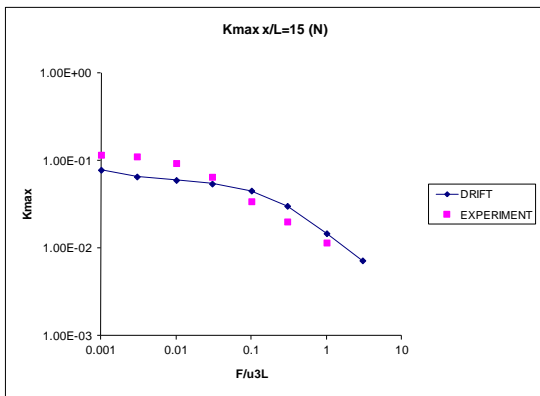
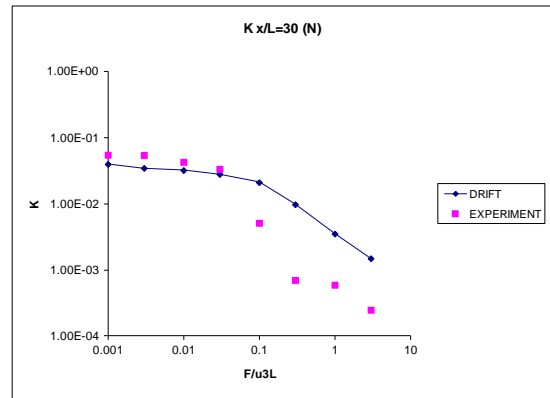
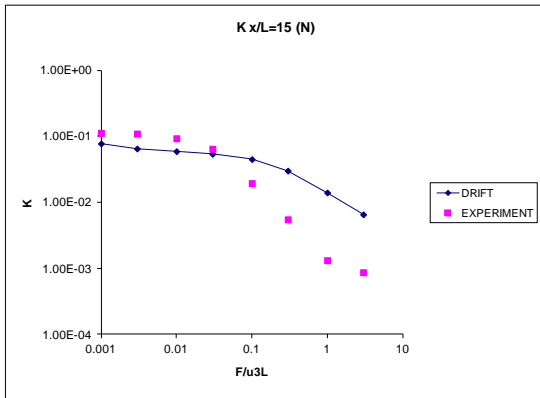
Source L



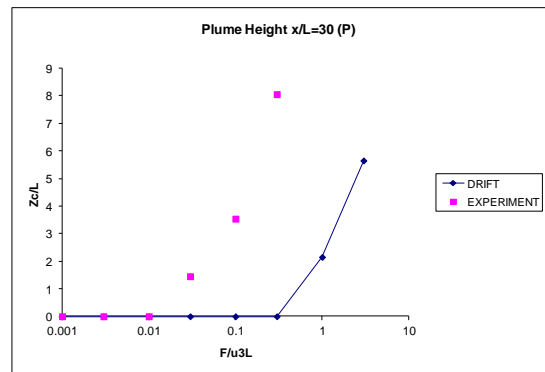
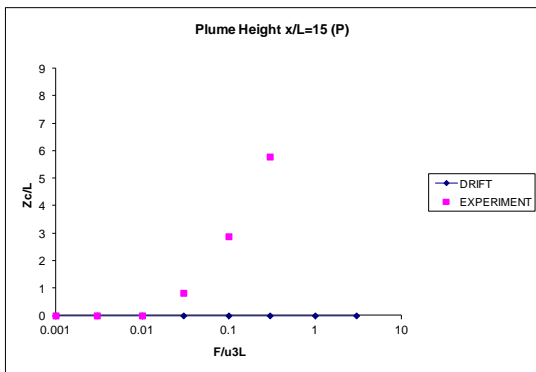
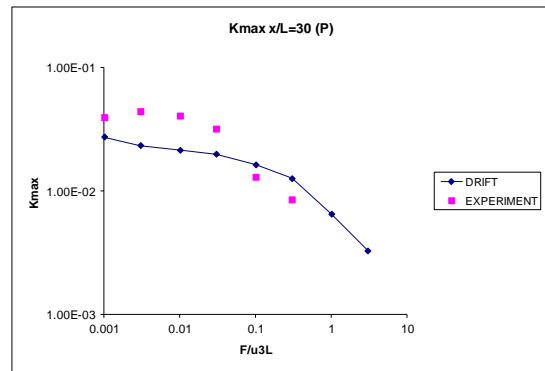
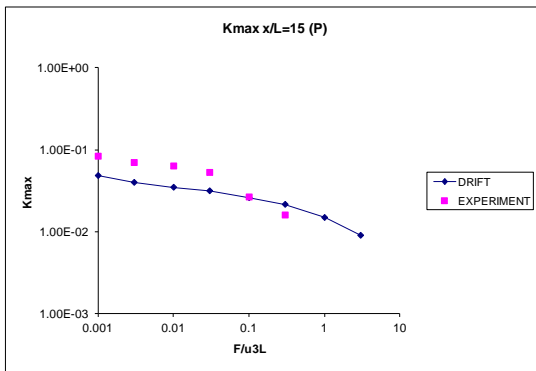
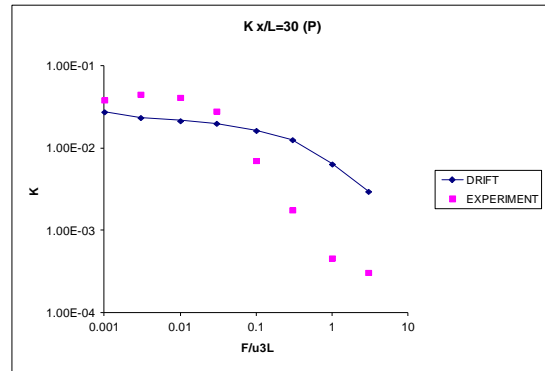
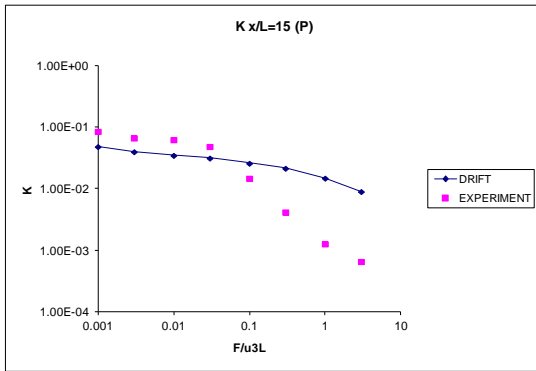
Source M



Source N

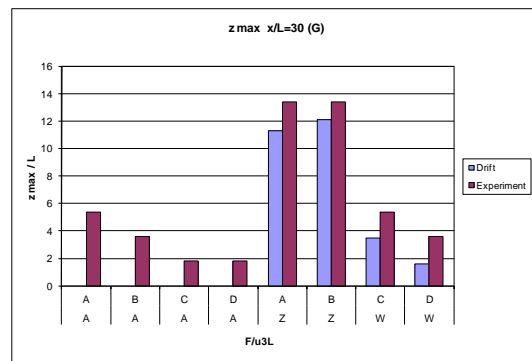
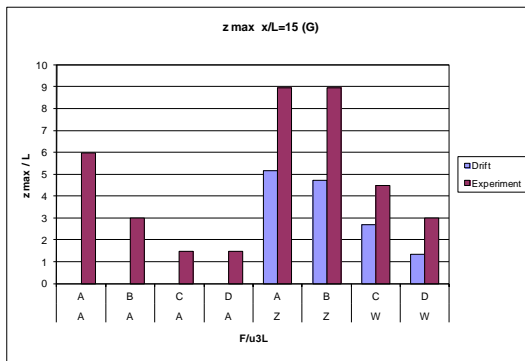
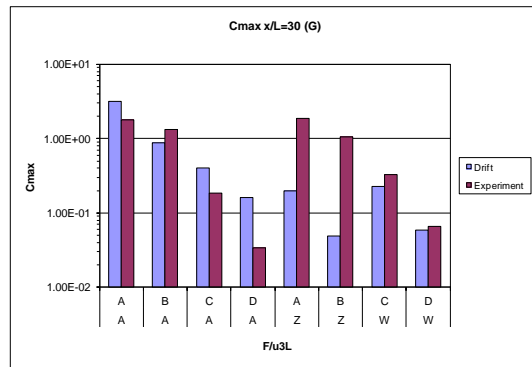
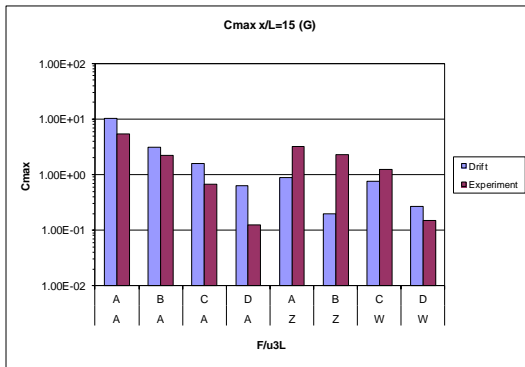
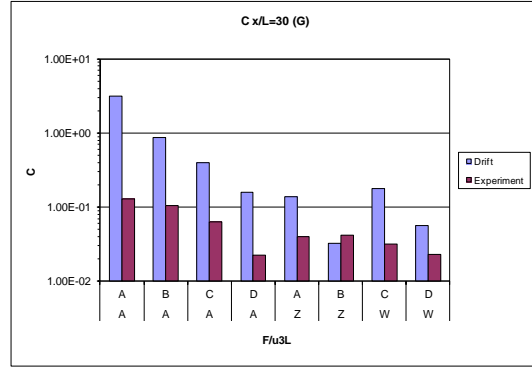
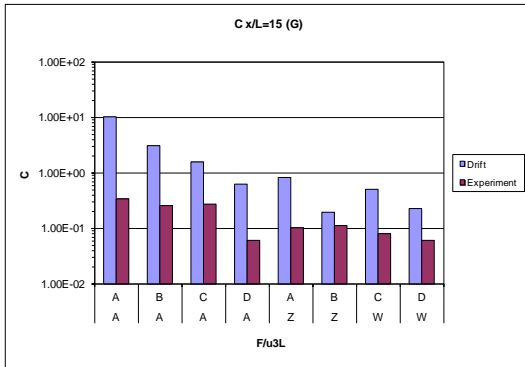


Source P

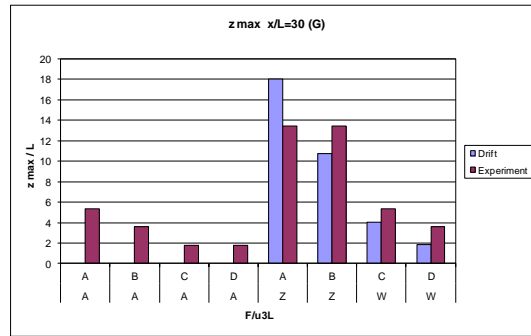
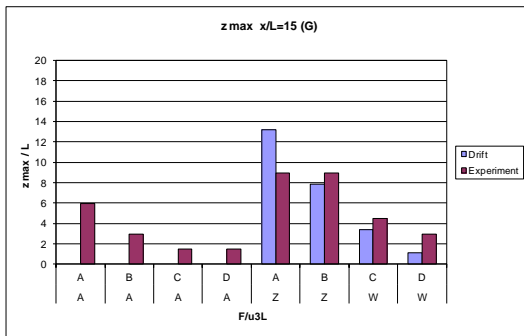
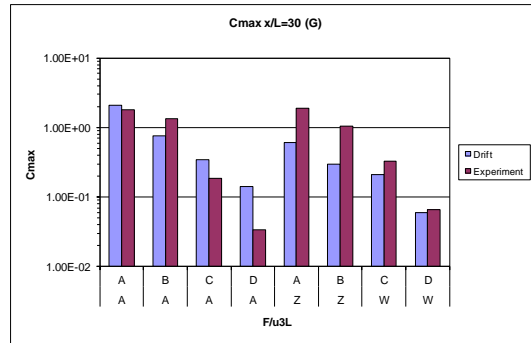
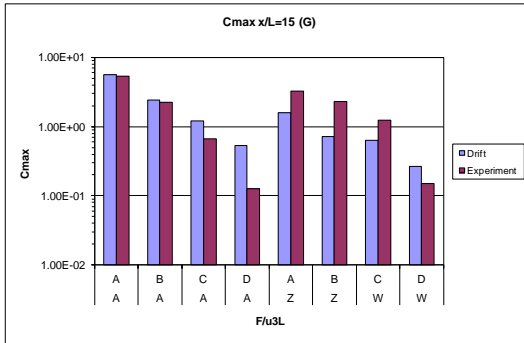
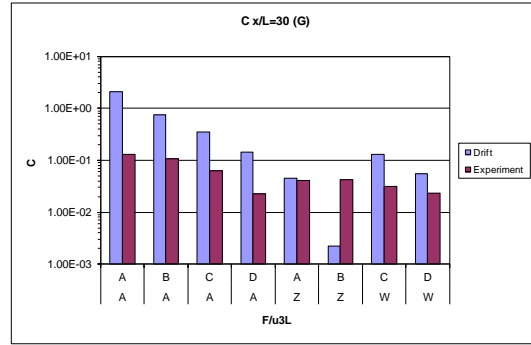
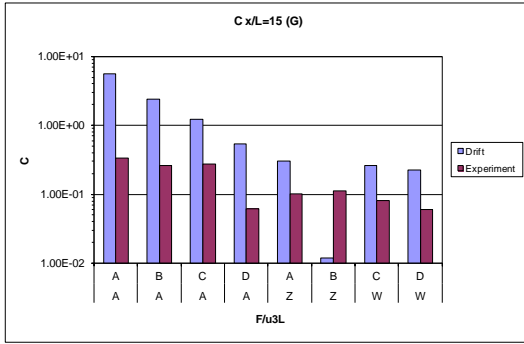


APPENDIX 2 BUOYANT PUFF GRAPHS

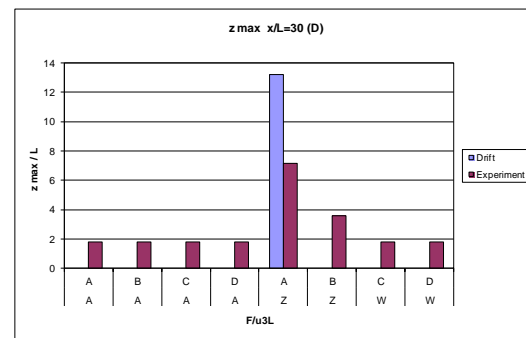
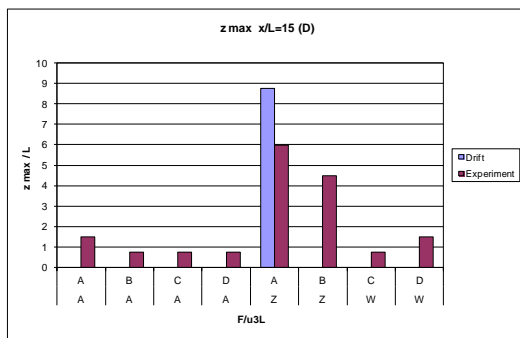
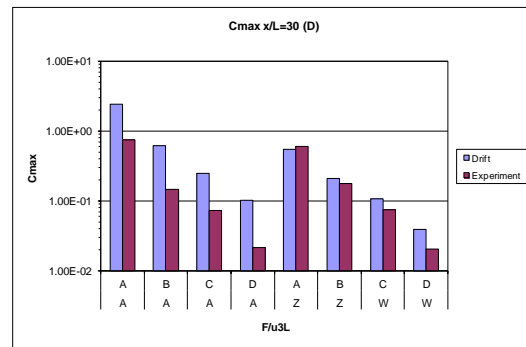
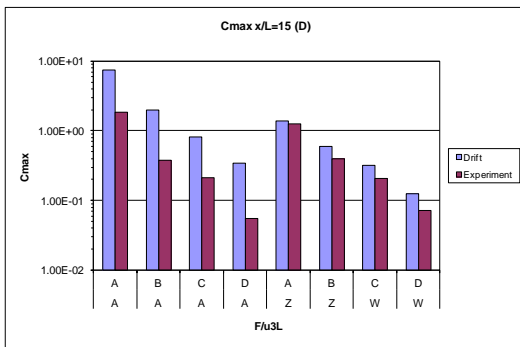
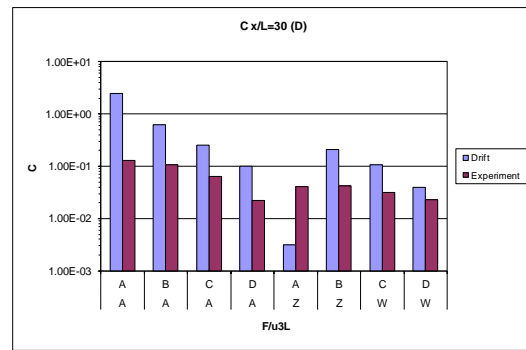
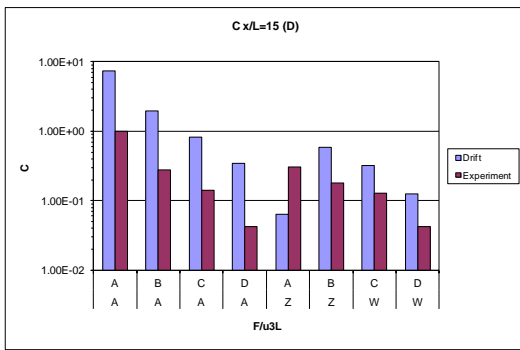
Source G: Finite Duration Model



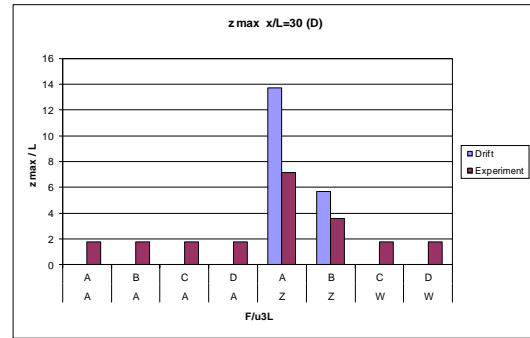
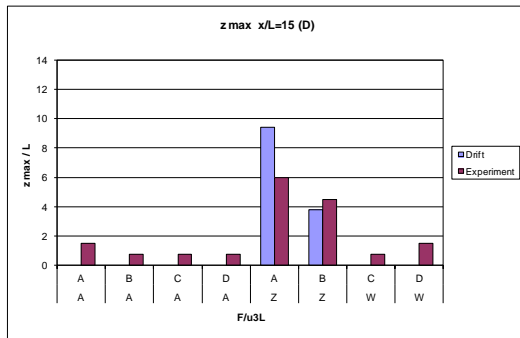
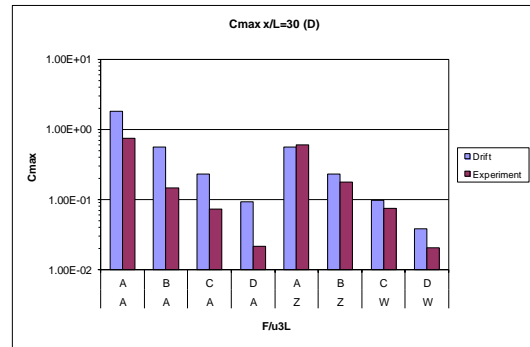
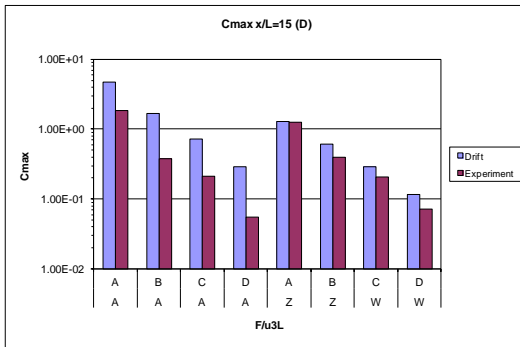
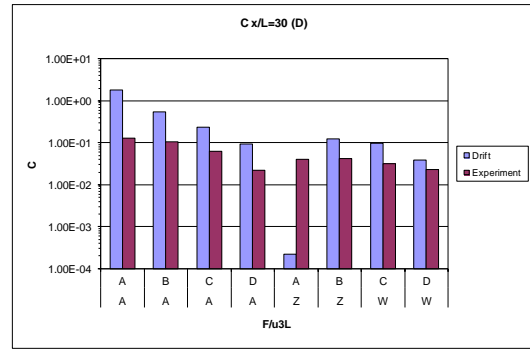
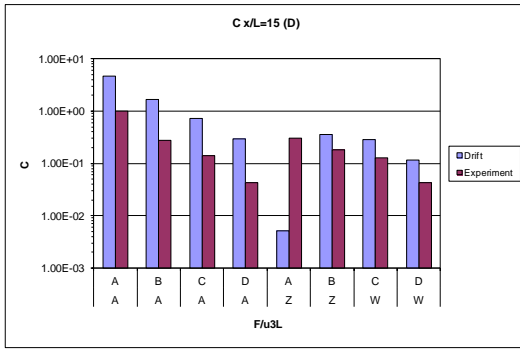
Source G: Instantaneous Model



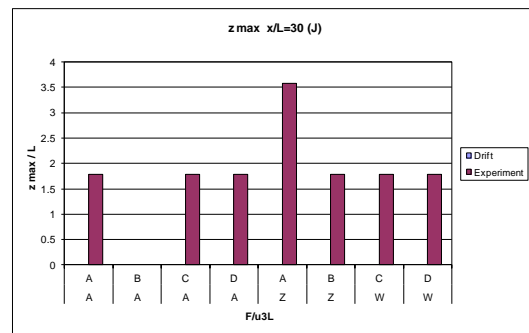
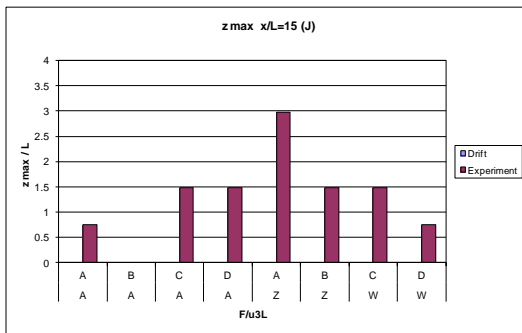
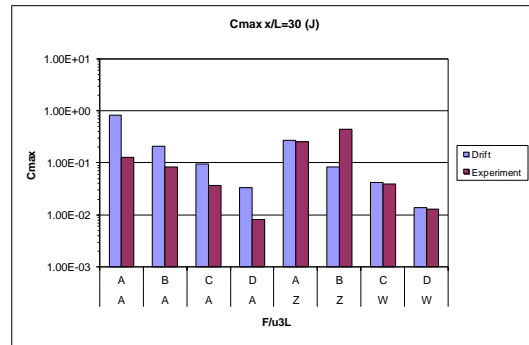
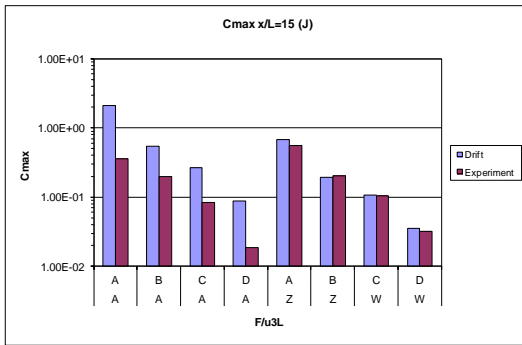
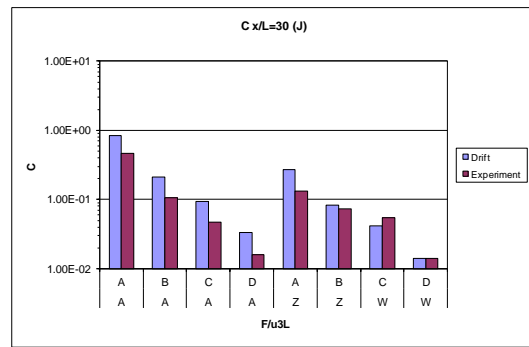
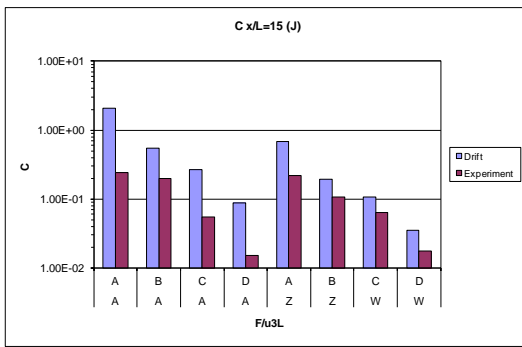
Source D: Finite Duration Model



Source D: Instantaneous Model



Source J: Finite Duration Model



Source J: Instantaneous Model

